1   **Atmospheric benzene observations from an oil and gas field in the Denver Julesburg basin in July**
2   **and August 2014**

3   Hannah S. Halliday[1], Anne M. Thompson[2,1], Armin Wisthaler[3,4], Donald Blake[5], Rebecca S. Hornbrook[6],
4   Tomas Mikoviny[3], Markus Müller[4], Eric C. Apel[6], Alan J. Hills[6]
5
6   [1]Department of Meteorology, The Pennsylvania State University
7   [2]Goddard Space Flight Center, Greenbelt, MD, USA
8   [3]Department of Chemistry, University of Oslo, Oslo, Norway
9   [4]Institute for Ion Physics and Applied Physics, University of Innsbruck, Innsbruck, Austria
10   [5]Department of Chemistry, University of California at Irvine, Irvine, CA, USA
11   [6]Atmospheric Chemistry Observations and Modeling, National Center of Atmospheric Modeling,
12   Boulder, Colorado, USA

13   **Abstract**

14   High time resolution measurements of volatile organic compounds (VOCs) were collected using a
15   quadrupole PTR-MS at the Platteville Atmospheric Observatory (PAO) to investigate how oil and natural
16   gas (O&NG) development impacts air quality within the Wattenburg Gas Field (WGF) in July and August
17   2014 as part of NASA's DISCOVER-AQ Colorado field campaign. The PTR-MS measurements at PAO
18   were supported by pressurized whole air canisters collected at the surface, vertical VOC measurements
19   made using an airborne PTR-MS Time Of Flight (TOF) instrument installed on the NASA P-3B aircraft,
20   and VOC measurements collected during the Front Range Air Pollution and Photochemistry Éxperiment
21   (FRAPPÉ) on the NSF/NCAR C-130. Unexpectedly high benzene mixing ratios were observed at PAO
22   (mean benzene = 0.53 ppbv, maximum benzene = 29.3 ppbv), primarily at night, and this high benzene is
23   associated with SW flow over the observation site. Vertical diurnal profiles indicate that the benzene is
24   originating the nearby environment, and source investigations conducted with tracers measured in the
25   pressurized canister samples implicate O&NG rather than urban benzene sources. A regional
26   toluene/benzene ratio analysis associated southerly flow over PAO with the Denver urban plume, and the
27   benzene/CO correlations are weak over all wind quadrants, indicating the urban emissions of benzene are
28   not responsible for the high observations at PAO. These results allow us to put a spatial constraint on the
29   source of the WGF benzene that has been measured in prior work at the Boulder Atmospheric Observatory
30   (BAO).

31   **Introduction**

32   Oil and natural gas (O&NG) extraction has been rapidly expanding in the Denver-Julesburg Basin
33   (DJB) in NE Colorado. In 2014 Colorado was ranked as the 5th highest state in number of gas wells, with
34   7.4% of the nation's wells located in Colorado. Colorado produced 5.2% of the total US natural gas
35   production in 2014. There are more than 25,000 active gas wells currently operating in the DJB, with the
36   greatest density operating in the Wattenburg Gas Field (WGF) in Weld County (COGCC, 2015). The area
37   has been drilled since the 1970's, but recent high natural gas prices have created a larger market and
38   incentivized natural gas development in the region. Increased unconventional extraction of oil and gas from
39   shale deposits in particular is a concern in the public health community (Colborn et al., 2011) and has been
40   shown to have an adverse effect on air quality in areas with heavy O&NG development (McKenzie et al.,
41   2012).
42   Ozone is a secondary pollutant that is produced from reactions between reactive nitrogen (NO +
43   $NO_2 = NO_x$) and VOCs under sunlight. The air quality impact of hydraulic fracturing has received

44 considerable attention from researchers and air quality managers because the Denver metro area and
45 Northern Front Range were categorized as non-compliant with National Ambient Air Quality Standards
46 (NAAQS) for ozone pollution in 2007, and the region has remained in marginal nonattainment through
47 2015 (Allison, 2015). Increased mixing ratios of volatile organic compounds (VOCs) have been attributed
48 to oil and gas activity in natural gas extraction basins, and these increased VOCs have been connected to
49 increased ozone (Katzenstein et al., 2003; Kemball-Cook et al., 2010; Petron et al., 2012; Gilman et al.,
50 2013; Moore et al., 2014; Warneke et al., 2014). The O&NG contribution to VOCs in the front range is
51 significant; the 2011 Environmental Protection Agency (EPA) National Emissions Inventory
52 (http://www.epa.gov/air-emissions-inventories/national-emissions-inventory) facility emissions reports
53 that 64% of the total point source VOC emissions in Colorado were attributable to O&NG extraction
54 activity, while in Weld County the O&NG contributions account for 90% of the total point source VOC
55 emissions.
56   Studies conducted within the DJB since 2011 have found a clear oil and gas signature in the VOCs
57 measured in the region, with enhancement in the alkanes and aromatics without corresponding increases in
58 combustion tracers (Petron et al., 2012; Gilman et al., 2013; LaFranchi et al., 2013; Swarthout et al., 2013;
59 Thompson et al., 2014). In addition to the effect of degrading air quality, high VOC concentrations are a
60 concern from a public health perspective. VOCs can be toxic to human health in their own right, especially
61 as emissions increase from human activities. Increasing mixing ratios of VOCs in heavy O&NG
62 development regions has been directly attributable to O&NG extraction, with sources coming from
63 infrastructure and transport, fugitive emissions, and deliberate venting and flaring (Adgate, 2014).
64 Increasing concentrations of methane, light alkanes, and aromatics in the DJB have been connected to
65 O&NG development (Petron et al., 2012; Gilman et al., 2013; La Franchi et al., 2013; Thompson et al.,
66 2014). Aromatics in particular are a public health concern, and the mix of benzene, toluene, ethylbenzene
67 and xylenes (BTEX) has been well characterized. BTEX has a wide variety of industrial uses as solvents
68 and feedstocks, and is released into the environment primarily through O&NG production and gasoline use
69 and storage (Bolden et al, 2015).
70   Exposure to aromatic VOCs has been linked to cancer, respiratory effects, and endocrine disruption
71 (McKenzie et al., 2012; Bolden et al. 2015). Benzene, the primary aromatic VOC, has a resonance stabilized
72 ring structure and an atmospheric lifetime of approximately 10 days, with the primary atmospheric sink
73 owing to oxidation by OH radicals. Benzene is classified as an air toxic under the USA Clean Air Act in
74 section 112, and is a known human carcinogen (IARC Group 1). Health effects associated with benzene
75 exposure include leukemia, anemia and other blood disorders and cancers, immune system impairment,
76 decreased respiratory function and neural tube defects in newborn babies (Bolden et al. 2015; McKenzie et
77 al. 2012). The effects on human health have been well documented in the literature, and benzene is one of
78 the better characterized air toxics. Although benzene emissions are not controlled through national
79 standards, exposure standards and guidelines have been set. However, exposure limits have generally been
80 defined for industry and acute exposure, which leads to high limits. The Occupational Safety and Health
81 Administration (OSHA) sets a general industrial permissible exposure limit of 1 ppm 8 hour time weighted
82 average, with a 5 ppm short term exposure limit. The National Institute for Occupational Safety and Health
83 (NIOSH) sets a lower short term 8 hour time weighted average of 0.1 ppm, with a short term exposure limit
84 of 5 ppm. The California Air Resources Board (CARB) literature sets the acceptable exposure limits much
85 lower, with an 8 ppb 6 hour exposure limit, and a 2 ppb 8 hour and chronic exposure limit. However, there
86 has been no safe threshold value for benzene exposure, and the EPA Integrated Risk Information System
87 (IRIS) assessment of benzene inhalation puts the excess carcinogenic risk from chronic exposure to benzene

88   at 1 in 100,000 for a chronic exposure of 0.41 to 1.41 ppbv benzene (1.3 to 4.5 µg/m^3 benzene). Since there
89   are uncertainties in the carcinogenic risk from benzene, the mean value of 0.877 ppb benzene for this excess
90   risk factor is used (2.8 µg/m^3 benzene).

91   Benzene is used as an anthropogenic tracer in VOC studies because it has a small number of well
92   characterized sources, with 78% of the benzene emissions in the EPA's 1996 National Toxic's Inventory
93   estimates attributed to mobile sources, mostly on-road. The remaining national benzene emissions are
94   attributed to the evaporation of fuels at service stations, solvent use, and oil and gas operations and
95   processing (Wallace, 1989; Bolden et al., 2015). Densely populated urban areas are the primary regional
96   sources of benzene due to traffic and industry emissions. Urban outflow studies have used benzene as a
97   tracer for urban influence in the rural environment (Roberts et al., 1984; Bravo et al., 2002; Seigneur et al.,
98   2003; de Gouw et al., 2005; Warneke et al., 2007; Apel et al., 2010). However, increasing oil and gas
99   production of aromatics means that while benzene mixing ratios have been dropping nationally (Fortin et
100   al., 2005), there is some evidence that benzene concentrations have been increasing outside of the urban
101   centers (Thompson et al., 2014). These gas field aromatic emissions have not been well characterized or
102   unambiguously identified. In Colorado a top down estimate of benzene over the WGF found that the official
103   inventories were too low by a factor of seven, and that the oil and gas emissions of benzene are on the same
104   order as the vehicle emissions for the region (Petron et al., 2014). A specific source for the natural gas
105   benzene was not definitively identified.

106   The present investigation, part of the 2014 NASA Deriving Information on Surface conditions from
107   Column and Vertically Resolved Observations Relevant to Air Quality (DISCOVER-AQ) field campaign
108   in July and August 2014, presents the first detailed analysis of benzene measurements made continuously
109   at a sampling site in the midst of O&NG activity in the WGF. The benzene data were collected along with
110   other VOCs by a PTR-MS at the Platteville Atmospheric Observatory, CO, one of six instrumented ground
111   stations in DISCOVER-AQ. Vertical benzene measurements were made using an airborne PTR-MS Time
112   Of Flight (TOF) instrument installed on the NASA P-3B aircraft which conducted regular spirals over
113   Platteville. Additional VOC measurements were collected concurrently during the Front Range Air
114   Pollution and Photochemistry Éxperiment (FRAPPÉ) on the NSF/NCAR C-130. From both surface and
115   aircraft we found unexpectedly high, possibly toxic, benzene levels under nighttime conditions. In the
116   following sections, we present the Platteville and aircraft benzene observations in detail to more completely
117   understand emissions from O&NG activities in the WGF. We address two main points in this study. First,
118   we examine benzene variability, which is characterized by comparison of aircraft data across the FRAPPE
119   region, over DISCOVER-AQ sampling sites, and at the Platteville surface site on a diurnal basis and over
120   three weeks of sampling. Second, we investigate potential benzene sources at the Platteville ground station,
121   using benzene data measured in canister samples and by the PTR-MS. Tracer correlations with benzene
122   and wind direction-benzene relationships measured at the site are used to identify general source locations
123   and likely O&NG activities contributing to the elevated benzene.

124   **Methods**

125   **Methods: Site Description**

126   NASA's DISCOVER-AQ field campaign was conducted from mid-July to mid-August of 2014 in
127   the Colorado Front Range region. The measurements encompassed the Denver urban region and the rural
128   gas field environment to the north of the Denver urban region bounded by Fort Collins, CO and the
129   Platteville Atmospheric Observatory (PAO). A map of the study area is shown in Figure 1. The campaign
130   measurements included six instrumented ground sites and two instrumented NASA aircraft (the P-3B and

131 the B200). This study primarily analyzes a subset of these measurements collected at the Platteville
132 Atmospheric Observatory (PAO) (40.1815 °N, 104.7268 °W). PAO was selected due to its central location
133 in the WGF, allowing the characterization of the gas field emissions. The site is located 9 km SE of the City
134 of Platteville (Lat: 40.214 °N, Long: 104.823 °W) and 25 km S of Greeley CO (40.422 °N, 104.709 °W).
135 The site elevation is 1520 m above mean sea level (ASL).

136 Air quality relevant trace gas sampling was made with a common inlet 4 meters above ground level
137 (AGL) within the Nittany Atmospheric Trailer and Integrated Validation Experiment (NATIVE) mobile air
138 quality research station (see Martins et al. (2012) for a full description). The NATIVE instrument package
139 provides one minute averaged *in situ* measurements of ozone, $NO/NO_2/NO_x$, total reactive nitrogen (NO_y),
140 sulfur dioxide (SO_2), carbon monoxide (CO), carbon dioxide (CO_2), and methane (CH_4). Additionally, one-
141 minute averaged meteorological data was also collected, including wind speed and direction, temperature,
142 relative humidity, pressure, and NO_2 photolysis rates.

Methods: PTR-MS VOC Collection

144 A conventional proton-transfer-reaction quadrupole mass spectrometer (PTR-QMS; Ionicon
145 Analytik, Innsbruck, Austria) was used for VOC measurements at the PAO site. The measurement principle
146 and technical details of this instrument have been reviewed in great detail elsewhere (DeGouw and
147 Warneke, 2007). Routine operating parameters and procedures were applied in this study. The drift tube
148 was operated at a pressure of 2.25 mbar, an electric field strength of 57 V/cm and a temperature of 50 °C.
149 The QMS was run in the multiple ion detection (MID) mode. It sequentially measured 51 m/z-signals over
150 the course of one minute. Benzene was detected as protonated benzene (m/z 79) with a 1-second signal
151 integration time during the 1-minute measurement cycle. The ethylbenzene interference with benzene
152 measurements was minimized (~25 % fragmentation on m/z 79). The interference from acetic acid (m/z 79
153 from hydrated protonated acetic acid) was found to be negligible.

154 A dynamically diluted certified multi-component gas mixture (Apel Riemer Environmental Inc.,
155 Broomfield, CO, USA) containing 1 ppmV of benzene was used for calibration. The instrumental
156 background was determined by supplying catalytically (Pt/Pd at 325 °C) cleaned air to the instrument. The
157 accuracy of the reported benzene volume mixing ratios is ±5.2%.

158 The PTR-QMS was housed at the PAO site in a separate trailer located 5 m from the NATIVE
159 trailer. Ambient air was sampled at a height of 5.6 m above ground (2.4 m above trailer roof) from a mast
160 attached to the trailer. The inlet line was a 6.25 mm outer diameter, 4.3 m long Teflon PFA tube that was
161 capped with a 5-6 □m pore size Teflon PTFE filter. The tube was heated to 40 °C inside the air-conditioned
162 trailer to prevent condensation. The flow rate through this main inlet line was 7 standard liters per minute
163 (slpm). The PTR-QMS subsampled from this flow.

164 A proton-transfer-reaction time-of-flight mass spectrometer (PTR-ToF-MS) was used for airborne
165 benzene measurements. This instrument and its operating procedures have been described in great detail by
166 Müller et al. (2014).

Methods: FRAPPÉ TOGA VOC Collection

168 The NCAR Trace Organic Gas Analyzer (TOGA), a fast on-line gas chromatograph/mass
169 spectrometer (GC/MS), was installed on the NSF/NCAR C-130 for the FRAPPÉ field study and made
170 continuous measurements of over 70 VOCs including benzene and toluene during the study. Integrated air
171 samples 35-s in duration were taken every two minutes and analyzed by TOGA in flight. For a detailed
172 description of TOGA, see Apel et al. (2015). The reported TOGA benzene and toluene data have an overall
173 uncertainty of ±15%, with detection limits of 0.5 pptV and 1 pptV for benzene and toluene, respectively.

174   **Methods: Canister Sample Whole Air VOC Collection**

175   The whole air canister samples were collected and analyzed by the University of California at Irvine
176   (UCI) VOC canister collection program. Modules of 12 stainless steel 0.9 liter canisters connected in series
177   with remotely operated valves. The fill time was ~30 seconds and the evacuated canisters reached final
178   pressures of ~10 psig. After the canisters were filled the modules were shipped to the UCI laboratory where
179   they underwent GC analysis for ~30 halogenated hydrocarbons and alkylnitrates and ~50 C2-C10
180   nonmethane hydrocarbons (NMHCs). The limit of detection (LOD) was 3 pptV for all NMHCs while the
181   halogenated gases/alkyl nitrate LODs ranged from 0.05 pptV to 10 pptV. For more details see Colman et
182   al., 2001.

183   **Methods: Ozonesonde Boundary Height Calculations**

184   Planetary boundary layer height (PBLH) calculations were made from ozonesonde profiles that
185   were collected at the PAO site. One to three ozonesonde-radiosonde profile pairs were launched each day
186   for a total of 42 total profiles. Boundary layer height was calculated from these profiles using the method
187   outlined in Martins et al. (2012). The profiles were smoothed by averaging the vertical data into 50 m bins,
188   and the lapse rate for defining the inversion was set at a minimum of 5 K/km. In addition we added the
189   criteria that the relative humidity did not change with altitude for these samples. If multiple possible heights
190   were selected with these metrics we used the lowest realistic value by inspection.

191   **Results**

192   **Results: Spatial Distribution of Benzene**

193   Six sites collected ground measurements during the campaign. Vertical measurements were made
194   by the P-3B flying spirals over the sites; each measurement location had two to three spirals per flight day.
195   VOC measurements were made with a PTR-MS Time of Flight (TOF) instrument, including benzene. To
196   determine the spatial differences of benzene measured over the sites we used the bottom one km AGL over
197   each site to calculate benzene statistics for the campaign. Figure 1 shows the mean benzene calculated for
198   each site are shown in context of the study area including the flight track taken by the aircraft and the
199   boundaries of the WGF. The anthropogenic sources of benzene lead to high mixing ratios at low altitudes,
200   so confining the statistical calculations to a single vertical km for each site allows us to assume that we are
201   comparing measurements that were primarily collected within the planetary boundary layer.

202   PAO shows the highest mean benzene over all spirals (0.140 ppbv), followed by Denver (0.119
203   ppbv) and the Boulder Atmospheric Observatory (BAO) (0.102 ppbv). PAO and BAO are both gasfield
204   sites, while Denver was the urban core. In comparison, the three sites closest to the mountains (Fort Collins,
205   Golden, and Chatfield) have low values relative to the gas field and urban sites. Fort Collins has the lowest
206   mean value during the campaign (0.068) ppbv) while the two sites expected to be most influenced by the
207   Denver Plume (Chatfield (0.080 ppbv) and Golden (0.087 ppbv) are slightly elevated relative to Fort Collins
208   but still low compared to Denver.

209   Table 1 shows the aggregate statistics for the six measurement sites. Putting the mean values into
210   context with the quartile values for each site shows that the means are relatively uniform, with Denver and
211   PAO in particular having close values despite the difference in environment. The two locations with the
212   highest observed values, BAO and PAO, are both gas field sites and are within the boundary of the WGF.
213   Benzene is expected to be high in the city center where vehicle emissions are the driver of anthropogenic
214   VOCs. Thus the high values in measured at the rural gas field sites are unexpected and indicate different
215   source influences on the observed benzene.

216   **Results: PAO Benzene Observations**

217   The time series of ground site benzene measured by PTR-MS during the campaign is shown in
218   Figure 2A. Figure 2B shows the daily benzene statistics, calculated from midnight to midnight local time
219   (MDT). The campaign diurnal cycle is shown in Figure 2C, and shows the extreme difference between the
220   daytime and nighttime data. The high nighttime benzene drives the high statistics over all measured days
221   in the campaign, Table 2. The diurnal split for the statistics is based on the suns position relative to the
222   horizon; the sun above the horizon was defined as daytime, and below the horizon was defined as nighttime.
223   During the daytime benzene mixing ratios are reduced and become less variable, while the nighttime
224   benzene shows much greater variability and the largest observed mixing ratios of the campaign. Beyond
225   the day/night diurnal split, Figure 2B also shows that there is some temporal variability in the observed
226   benzene, with the later third of the campaign from 31 July to the end of the observations on 08 August
227   having higher nighttime benzene.

228   The benzene measured at PAO was higher than expected for the region. Canister samples collected
229   in the City of Platteville in 2013 saw peak benzene of 0.96 ppbv (Thompson et al. 2014), well below the
230   2014 PAO maximum of 29 ppbv. While some of this disparity is explained by the differences in sample
231   techniques and the fact that the samples in Thompson et al. (2014) were collected between 0600 and 0900
232   MST, the difference in the benzene range was unexpected. The benzene levels measured at PAO during the
233   2014 campaign are high enough to be problematic from a health and welfare standpoint. The fact that these
234   high benzene mixing ratios mostly occurred at night, when canister samples are not routinely collected in
235   this region, means that the canister studies previously conducted in the WGF did not capture the full range
236   of the benzene exposure.

237   Figure 3 shows the benzene relationship to PBLH, calculated from both the ozonesonde-radiosonde
238   profile pairs and MPL aerosol data. The surface benzene concentrations are sensitive to the planetary
239   boundary layer height (PBLH), especially in the early morning and late evening when the PBLH is low but
240   the sun is still above the horizon. Under these conditions the boundary layer has a stable inversion structure,
241   which prevents vertical mixing and keeps any ground level emissions of VOCs close to the earth's surface,
242   driving up mixing ratios at the surface. Benzene mixing ratios are enhanced when the PBLH is shallow, but
243   as convective mixing begins and the PBLH begins to grow, the benzene mixing ratios drop off. Once the
244   PBLH is greater than 0.5 km above ground level (AGL) the benzene mixing ratios level off and approach
245   the daytime median benzene value.

246   The MPL PBLH measurements generally agreed with the ozonesonde PBLH measurements
247   collected at the site. The mean and median MPL PBLH begin growing at 0900 MDT and level off between
248   1700 and 1900 MDT (Supplementary Figure 1). At 1000 MDT both the mean and the median of the MPL
249   PBLH are $\geq$ 0.5 km AGL, which is the PBLH height where benzene stops being sensitive to PBLH. After
250   1900 MDT the MPL PBLH can continue to increase, but since this method uses aerosols to define the
251   boundary layer, these measurements can be unreliable. Aerosols lofted into the troposphere as the PBLH
252   grows will remain in the troposphere even when the PBLH collapses, which makes determining the true
253   nighttime PBLH difficult or impossible using the MPL.

254   **Results: Aircraft Comparisons**

255   The ground observations at PAO were supported by vertical profiles sampled by PTR-MS of the
256   P3B aircraft, collected by spirals conducted in a top-down approach over the site, with the aircraft starting
257   high and ending at low altitude. An overview comparison between the benzene measured on the P3-B and
258   the ground instrument is shown in Supplementary Figure 2. Flights occurred over the PAO between the

259   hours of 0800 and 1600 MDT throughout the campaign with two to three full profiles scheduled on each
260   flight day. A total of 32 full vertical profiles were completed over PAO during the campaign.

261   <u>Figure 4</u> shows the diurnal pattern of benzene measured in the vertical columns and on the ground,
262   faceted by hour of day binned vertically by 50 m sections. The overall mean vertical profile is shown in
263   <u>Supplementary Figure 3</u>. In the early morning hours the benzene measured on the ground is high, with low
264   benzene in the aircraft measured column. As the day progresses and mixing in the boundary layer begins
265   two trends begin: first, the ground measured benzene decreases, second, the benzene in the column
266   increases. A clear benzene boundary layer can be observed in the vertical benzene measurements growing
267   throughout the morning and midday. By midafternoon the troposphere is well mixed with respect to
268   benzene.

269   The high ground benzene at PAO coupled with the low benzene mixing ratios in the early morning
270   spirals indicates that a pool of benzene builds overnight at the surface. The benzene emitted into the low
271   boundary layer overnight is mixed up into the troposphere as the boundary layer grows, causing the mean
272   benzene to fall with height. Similar decreases of benzene concentration with height were observed at BAO
273   in 2011 (Swarthout et al. 2013), and attributed to local emissions of gas field benzene. The diurnal profiles
274   indicate that the high benzene comes from the surface, and this indicates advection aloft is not a significant
275   contributor to the benzene measured in the columns.

276   **Results: Benzene Polar Frequency Analysis**

277   To get more information on potential sources, we used polar frequency analysis of the surface
278   measured benzene at PAO. These plots use wind speed and direction information to determine how wind
279   regimes are associated with the high benzene observations. The wind speed and direction data was binned
280   by 10 degrees wind direction and 0.5 m/s wind speed, and statistics on the associated benzene observations
281   are calculated for each bin independently. The full campaign polar frequency plots are presented in <u>Figure</u>
282   <u>5.</u> Benzene is associated with W and SW wind flow, with the highest mixing ratios originating from the
283   southwest in a confined wind regime.

284   Separating the polar frequency plots into median (Fig. 5a), mean (Fig. 5b) and maximum (Fig. 5c)
285   allows us to investigate the directional dependence of the enhanced benzene at different mixing ratio levels
286   – low and background through the median, mid-level through the mean, and the wind regimes associated
287   with the highest benzene through the maximum. In all three polar frequency plots the benzene is associated
288   with SW flow. A westerly enhancement in the median plot is most likely due to mountain-valley circulation
289   over the site, but the persistent SW enhancement of benzene to the SW in all three polar frequency plots
290   indicates a primary benzene source SW of PAO. Although there is not a distinct point source, the high
291   benzene observed at PAO has a directional component; it is not simply a general elevation of mixing levels
292   throughout the region.

293   **Results: Canister Correlations and VOC Influences at PAO**

294   To assess the general influence of VOC sources at PAO we use four O&NG VOCs that correlate
295   with the O&NG and urban tracers, propane and acetylene: i-pentane, n-pentane, n-butane, and ethane. All
296   four of the tracer species are primarily emitted from natural gas, but can also be sourced from traffic
297   combustion in small amounts (Gentner et al. 2013; Thompson et al. 2014). The results are shown in <u>Figure</u>
298   <u>6a and 6b.</u> The canister sample correlations of the four tracer species with propane are strong, with i-pentane
299   ($R^2 = 0.985$), n-pentane ($R^2 = 0.971$), n-butane ($R^2 = 0.992$) and ethane ($R^2 = 0.936$), showing excellent
300   correlation over all 35 samples. In contrast, the correlations with acetylene are much weaker; i-pentane (R^2
301     $= 0.492$), n-pentane ($R^2 = 0.434$), n-butane ($R^2 = 0.504$) and ethane ($R^2 = 0.424$). The tracer correlations

302 presented in our study agree very well with the correlations of benzene and propane that are reported in
303 Thompson et al (2014), a study conducted with canister samples collected by the CDPHE in the city of
304 Platteville in 2013. Strong correlations with acetylene would indicate that the Denver plume is the most
305 important VOC source due to the heavy traffic influence in the urban center, but the propane correlations
306 are exceptional and indicate that PAO was heavily influenced by O&NG activity in 2014 during
307 DISCOVER-AQ.
308   The comparison of Thompson et al (2014) to the PAO canister samples is presented in Table 4; this
309 comparison study is currently the best published comparison of VOCs and correlations for non-BAO
310 measurements in the WGF. Our reported correlations with acetylene agree in general with Thompson et al
311 (2014), although our R^2 values are much higher. There is far less acetylene measured in the canister samples
312 at the PAO, which is isolated from major traffic, compared to the City of Platteville, which straddles US
313 85, a N-S highway with heavy truck traffic. Conversely, propane is expected to have higher mixing ratios
314 at PAO due to its location centered in the gas field; this is verified in the observations.
315   While the VOC/tracer correlations in Figure 6a and 6b indicate that an O&NG source important
316 for benzene at PAO, we wanted to quantify this relationship for the benzene samples. The high benzene
317 measured at PAO coupled with the vertical diurnal profile, Figure 4, and the directional dependence, Figure
318 5, indicates that benzene originates from some kind of anthropogenic activity from the SW of PAO. To
319 better identity the primary benzene source, tracer species well characterized for atmospheric sources are
320 analyzed. Commonly used compounds in O&NG studies include the VOCs propane, an O&NG tracer, and
321 acetylene, a traffic and urban tracer. These tracer compounds are not measured by PTR-MS, but pressurized
322 canister samples collected at PAO during the P3-B spirals were analyzed for these tracers. Note, however,
323 that the canister samples are confined to daylight observations.
324   Benzene was collected in both the canister sample and by the PTR-MS, and these two techniques
325 had excellent agreement over the measurement period (Supplementary Figure 4). Using a two minute
326 average centered at the time of canister opening to accoung for the slight separation of the instruments
327 returned a correlation slope of slope of 1.007 ppbv PTR-MS benzene/ppbv canister benzene and an R^2 value
328 is 0.921. Figure 6c and 6d show the results of correlating canister and PTR-MS benzene to propane and
329 acetylene measured in the canisters. The correlations with propane (Figure 6c) are moderately correlated
330 (canister benzene to canister propane, $R^2 = 0.782$; PTR-MS benzene to canister propane, $R^2 = 0.700$), and
331 indicate that there may be some common source. In contrast the correlations with acetylene (Figure 6d) are
332 very weak (canister benzene to canister acetylene, $R^2 = 0.375$; PTR-MS benzene to canister acetylene, R^2
333 $= 0.272$). The benzene correlations with acetylene and propane are comparable to literature values collected
334 in the City of Platteville reported in Thompson et al. (2014), which found that benzene correlated with
335 propane ($R^2 = 0.73$) much more strongly than to acetylene ($R^2 = 0.29$).
336   In emissions budgets benzene is primarily attributed to combustion emissions. The CDPHE keeps
337 a bottom-up emission inventory based on permit data and empirical calculations, and the 2011 inventory
338 assessments assigned nearly 90% of the total front range benzene emissions to vehicles, both highway and
339 nonroad (Petron et al. 2014). Benzene has been quantified in the WGF by three papers: two studies at BAO
340 (Petron et al. 2012; Gilman et al. 2013), and the Thompson et al. (2014) study in the City of Platteville.
341 These studies indicate that benzene Platteville has contributions from both traffic and non-combustion
342 evaporative sources. While these studies did not quantify the source contributions on the ground, a top
343 down estimate of benzene over Weld County was seven times higher than the CDPHE inventory estimates
344 of benzene emissions for the same region (Petron et al. 2014). They conclude that the benzene emissions
345 from evaporative sources over the WGF are on the same order of magnitude as the vehicle emissions, and

346 that mismatch between the top down measurements and the state inventory assessment is consistent with
347 missing benzene emissions in the Colorado Front Range Region. The assertion that the benzene evaporative
348 emissions could be equal or greater than the vehicle emissions is substantiated by the correlation results
349 that we see in our work, with the propane tracer having a stronger correlation to benzene than acetylene.
350   The isomers of pentane, i-pentane and n-pentane can be used as additional tracers for distinguishing
351 traffic from natural gas sources. Tailpipe emissions enhance i-pentane, so the i-pentane/n-pentane is used
352 as a fingerprint to discriminate urban vs natural gas VOC sources. High ratios of i-pentane/n-pentane
353 indicate urban and traffic sources, whereas lower ratios are a fingerprint of O&NG sources. Furthermore,
354 these are affected equally by atmospheric mixing and dilution and by photochemical processing, so the
355 source ratios remain constant (Gilman et al. 2013). A comparison of the PAO observations to published
356 values is shown in Figure 7. The canisters collected at PAO in July and August 2014 have a i-pentane/n-
357 pentane ratio of 0.888 (R^2 = 0.9885), a value close to the ratio of 0.86 reported for raw natural gas in the
358 WGF (CDPHE, 2007). Other studies in NE Colorado have found similarly low ratios: 0.885 at the BAO in
359 2011 (Gilman et al. 2013), 0.965 in Longmont CO (Thompson et al. 2014), and 1.00 at BAO (Swarthout et
360 al. 2013). In contrast, fresh vehicle emissions have a ratio of 2.96 (Broderick and Marnane, 2002).
361 Measurements taken in Denver, CO, and Boulder, CO, show a greater influence from the fresh vehicle
362 emissions, with Denver having a reported ratio of 1.87 (Baker 2008), and Boulder recording 1.10 (Gilman
363 2013). PAO is dominated by O&NG influence during the day when both urban/vehicle and O&NG
364 emissions can influence the site.
365   A final correlation between i-butane and n-butane was calculated, which returned a campaign ratio
366 of 0.405 (R^2 = 0.993). This ratio is in general agreement with the i-butane to n-butane ratios measured by
367 Swarthout et al. (2013) and Thompson et al. (2014), respectively 0.41 and 0.43, and to measurements
368 collected by the CDPHE (2012), 4.2 ± 0.03. These regional ratios are comparable to measurements in well
369 mixed urban and rural regions (Parrish et al., 1998; Watson et al., 2001), but lower than the ratio expected
370 for vehicle emissions or gasoline (Conner et al., 1995; Jobson et al., 2004). Emissions from commercial
371 natural gas have measured i-butane/n-butane at 0.60 (Fujita, 2001), but butane ratios this high have not
372 been recorded in the WGF, indicating that the natural butane ratio for this gas field are naturally around
373 0.4.

Results: Toluene/Benzene Ratios

375   Toluene is co-emitted with benzene with source dependent ratios. Toluene photolyzes more rapidly
376 than benzene under ambient conditions and the ratio of these two compounds can be used to assess the
377 photochemical processing of an airmass; a lower ratio of toluene to benzene indicates an aged airmass
378 (Roberts et al. 1984). In idealized urban outflow scenarios a photochemical clock calculation performed
379 with benzene and toluene can be used to calculate an effective airmass age. However, these calculations
380 don't work reliably in areas where there are additional non-vehicle emissions of the aromatic compounds
381 (Gelencser et al. 1997), such as in the WGF. However, these calculations can still be useful for identifying
382 and separating observations at PAO. Fresh emissions from gasoline evaporation and vehicles without
383 catalysts have a toluene/benzene ratio ≥ 2 (Barletta et al. 2002; Heeb et al. 2000; Bravo et al. 2002), and
384 the mean ratio for the Denver urban region was measured as 2.1 (Baker, et al 2009). A spatial map of the
385 toluene/benzene ratio calculated from the C-130 TOGA instrument, Figure 8, shows that using a
386 toluene/benzene ratio cutoff of 2 or greater is appropriate for differentiating the urban environment from
387 the surrounding rural environment.

388   The spatial toluene/benzene analysis presented in Figure 8 offers context on both the ratio analysis
389   as well as the spatial distribution of benzene in the study area. This plot encompasses all data collected
390   during the Frappé field campaign (27 July 2014 to 18 August 2014) to offer a broad context for the
391   observations. The points are colored by the toluene/benzene ratio cut off value of 2, but the points are sized
392   by the magnitude of the benzene observation for each point. The highest benzene of the campaign is
393   measured within the boundary of the WGF, but these high observations occur on the W side of the Greeley
394   urban area as well as in the SW corner of the WGF just to the north of the Denver urban boundary. While
395   PAO has high benzene measurements through the P-3B observations and ground observations, the TOGA
396   data shows that PAO is associated with comparatively low values. This is both evidence of the value of
397   ground measurements, especially at night, as well as some additional evidence for a benzene source located
398   to the SW of PAO. Interestingly, the highest benzene observations are not associated with NE flow over
399   the site despite the high benzene values over Greeley, CO. This is explained by the flow characteristics over
400   PAO, where SW flow is more likely (Figure 4D), and the Greeley, CO, emissions are not advected strongly
401   to the SW to affect PAO.

402   Figure 9A shows the correlation of benzene to toluene for all PAO PTR-MS observations taken
403   during the campaign; the data with a toluene/benene ratio ≥ 2 has been colored. This high ratio of
404   toluene/benzene only accounts for 5% of the total benzene observations; furthermore, these observations
405   are a distinct lobe of the correlate plot. When the maximum values viewed spatially in a polar frequency
406   plot (Figure 9B) it is clear that these high values are originating from due south of PAO, an area that is not
407   associated with the elevated benzene.

408   A previous study done at BAO used the toluene/benzene ratio separated by wind sector to attribute
409   emissions types in each sector (Swarthout, 2013). This study also found the highest mean toluene/benzene
410   ratios to the south (1.09 ± 0.40), and attributed the source to regular impact from the Denver plume. Lower
411   ratios of toluene/benzene in the NE sector (0.76 ± 0.25) are attributed to O&NG emissions. When the mean
412   toluene/benzene ratio is calculated by wind sector for PAO (Table 3), we also see the highest ratios
413   associated with southerly winds (1.41 ± 1.86). This result, coupled with the polar frequency analysis of the
414   max toluene/benzene ratio, Figure 9B, indicates that a recently emitted urban signal is sourced from south
415   of PAO and the high benzene signal from the SW is not associated with the Denver plume. This is an
416   important result. The high benzene measured in the WGF at PAO clearly originates from local gas field
417   sources, and is not due to urban outflow.

418   The full list of the toluene/benzene ratios are in Table 3. The ratios show a distinct diurnal pattern
419   from all wind directions, with higher ratios observed at night in all sectors. The lowest mean ratios are
420   observed in the E and SE wind sectors but these two sectors are also associated with the lowest mean values
421   of both benzene (E = 0.28 ± 0.36 ppbv, SE = 0.20 ± 0.25 ppbv) and toluene (E = 0.35 ± 0.55 ppbv, SE =
422   0.25 ± 0.37 ppbv). This is in contrast to Swarthout (2013), who observed their depressed toluene/benzene
423   ratios occurring in the NE in association with increased aromatics. The PAO observations show
424   approximately equal value toluene/benzene ratios from all sectors, including during calm winds (wind
425   speeds < 1 m/s). These high ratio values compared to Swarthout et al. (2013) and the uniformity with
426   respect to wind direction indicates that there is considerable directional impact from the Denver urban
427   plume at PAO. However, when it does occur it is associated with S rather than SW flow.

428   **Results: Benzene and CO Relationship**

429   The previous WGF benzene studies at BAO used correlations with CO to differentiate benzene
430   sources (Petrone et al., 2012; Swarthout et al., 2013). Urban emissions of benzene are correlated with CO

431   due to their major common source in vehicle exhaust; at BAO benzene originating from the southern wind
432   sector correlates well with CO ($R^2 > 0.8$ for S wind sector). Both of these studies also identified enhanced
433   aromatics in the NE wind sector; the benzene/CO slopes were enhanced while the two species were still
434   correlated ($R^2 = 0.58 – 0.86$).
435   When the benzene/CO correlations are calculated for the PAO data over all observations, the R^2
436   value of 0.099 suggests no correlation. Both benzene and CO have a strong directional component (Figures
437   4 and 10), and both species have their highest correlations from SW of the site. However, there is no
438   directional dependence in the correlation of benzene and CO over the campaign; even in the SW wind
439   sector, high benzene occurs during low CO measurements.
440   High benzene without a corresponding CO source is observed from all wind sectors, which can be
441   explained by an O&NG benzene source. In contrast, elevated CO is associated exclusively with the SW
442   wind regime (Figure 10). While benzene and CO do track occasionally, as expected for a vehicle or urban
443   source, often these two species occur independently. The directionally dependent correlations of CO and
444   benzene are shown in Figure 11. There are three major benzene/CO regimes observed during the campaign:
445   benzene and CO tracking from a common traffic or urban source, benzene increases without associated CO
446   increases, and CO increases without associated benzene.
447   The highest independent CO and benzene observations are observed from the same SW wind
448   sector, but they are independent in time, indicating that there are two separate sources for these important
449   molecules that are both located in the SW. The tightly constrained wind regimes associated with high CO
450   and the lack of correlation with benzene indicates that it's unlikely these high CO values originated from
451   either the Denver urban area or from major freeways to the W and SW of PAO. Instead, it seems more
452   likely that we observe a stationary CO source and a separate temporally variable benzene source, both
453   located in the same general region to the SW of PAO.
454   In Colorado CO emissions have been attributed gasoline vehicles (66%) and non-road gasoline
455   powered equipment (26%) (LaFranchi et al. 2013). The remaining emissions are attributed to a variety of
456   processes, including industrial activity and natural gas processing. The extremely high observed mixing
457   ratios of CO coupled with the lack of a correlation with benzene or other tracers indicates that a close range
458   CO production is not associated with vehicle emissions.

459   **Discussion: Potential Sources of Benzene**

460   If the high benzene observed at PAO was primarily from the Denver metropolitan area we would
461   expect to see it correlate strongly to the combustion tracers, acetylene and CO (Bourbon et al. 2013; Apel
462   et al. 2010). However, we see weak and non-existent correlations over the full campaign for these species.
463   In addition, the highest benzene occurs with low CO mixing ratios. High benzene that is not correlated with
464   vehicle combustion tracers has been observed in areas with heavy industry, such as Houston TX (Gilman
465   et al. 2009). O&NG emissions of benzene are expected to correlate better with other O&NG VOCs, such
466   as propane and ethane. Studies in areas of heavy O&NG production have shown this behavior, especially
467   for sites associated with natural gas production (Helmig et al. 2014; Petron et al. 2014, Warneke et al. 2014).
468   Observational work conducted at BAO has found anomalously large benzene mixing ratios from
469   the NE, which they attributed to general O&NG production in Weld county (Petron, et al. 2012; LaFranchi
470   et al. 2013, Swarthout et al. 2013). However, further specification of the exact source of the high benzene
471   has not been made, except to assume that there is a mix of automotive and natural gas sources in the WGF.
472   A separate source of urban benzene was measured from S and W of BAO. The measurements taking at
473   PAO for our 2014 work are based much deeper in the WGF and are NE of the BAO tower. At PAO the

474   highest measurements of benzene come from the SW, indicating that the source of high benzene measured
475   from the NE in the BAO papers is located somewhere in between the BAO and PAO sites. The SW quadrant
476   is influenced by a mix of air sourced from vehicle exhaust as well as from this unidentified benzene source,
477   resulting in the highly uncorrelated benzene/CO behavior that we observe.

478   Our observations, along with the BAO observations (Petron, et al. 2012; LaFranchi et al. 2013,
479   Swarthout et al. 2013), confine the high benzene to a smaller geographic area within the WGF. In addition
480   to a narrowed source area we also know that the benzene mixing ratios are highly variable, especially at
481   night, indicating that a transient source related to O&NG production is operating near PAO. Benzene
482   emissions have been a concern in upsteam gas production, and VOCs have been identified as emissions for
483   various parts of the natural gas extraction process. Specifically, these processes are 1) diesel vehicle
484   emissions; 2) gas flaring and deliberate venting; 3) drilling flowback of waste mud and water; 4) fugitive
485   emissions from infrastructure and maintenance; 5) condensate tanks (Adgate et al. 2014; Verma et al. 2000;
486   Buzcu-Guven et al. 2013).

487   The benzene observations do not correlate with formaldehyde measurements ($R^2 = 0.003$) at PAO;
488   these formaldehyde measurements were made with the PTR-MS on the surface at the observation site. A
489   correlation could have indicated a flaring source (Knighton et al. 2012), which has been identified as a
490   benzene driver in Texas (Buzcu-Guven et al. 2013). Our tracer correlations eliminated traffic and urban
491   sources as well. This leaves the most likely potential O&NG sources as one of four potential options:
492   drilling flowback, gas venting during production or pipeline maintenance, fugitive emissions from
493   infrastructure, or emissions from condensate tanks.

494   Drilling flowback and waste water is stored in temporary waste pits at the drilling sites (Colborn et
495   al. 2011), the locations of which are monitored and reported by the Colorado Oil and Gas Conservation
496   Commission (COGCC). Regulatory advances have phased out this type of storage in favor of closed
497   systems (CDPHE, 2012), but active locations are still recorded in the WGF by the COGCC. There is a
498   dense group of these pits located between PAO and BAO (Supplementary Figure 5). While many of these
499   are inactive locations, meaning decommissioned and buried, a large number of them have an unknown
500   status. Additionally, a number of the active pits are located west of PAO, which is associated with high
501   mean and median benzene mixing ratios and low mixing ratios of CO. However, produced water and
502   drilling waste has not been identified with high atmospheric benzene concentrations in previous studies
503   (Bloomdahl et al., 2014; Bunch et al., 2014), although published atmospheric measurements of these waste
504   pits are difficult to locate. Environmental impacts from these waste pits are more likely to be associated
505   with poor water quality (Eiceman et al., 1986; Gross et al., 2013)

506   While we've rejected flaring as a significant source of benzene based on the correlations between
507   benzene and formaldehyde, the proximity of O&NG facilities to air quality monitoring stations has been
508   shown to increase measured benzene levels; gas plants < 50 km from the measurement sites were shown to
509   have a statistical increase for benzene, although a mechanism was not hypothesized (Bursyn et al. 2007).
510   PAO was located 4.5 km to the NE of the Platte Valley Gas Plant, which is owned by DCP Midstream LP
511   and was operational through our study period. Fugitive VOC emissions, including benzene and toluene, are
512   expected in refining facilities, mostly from storage tanks and poor seals, but also from conversion and
513   treatment processes (Rao et al., 2005). In oil refineries the coker unit has specifically been implicated (the
514   process cracks long chain hydrocarbons into shorter molecules), along with the storage areas for the raw
515   feedstock and final product tanks (Chambers et al. 2008). Natural gas processing does not have a coking
516   process, but leaks from storage containers may be a significant source of VOCs from the processing plant
517   (Bar-Ilan et al., 2008).

518   Condensate tanks have been implicated in gas field VOC emissions in previous studies (Moore et
519   al., 2014). In exposure studies of upstream natural gas, the gas dehydrator units are implicated as the largest
520   single factor of exposure for workers (Capleton and Levy, 2005). Flashing emissions from these units have
521   been estimated to produce about 65% of the total natural gas extraction VOCs in Colorado (Pertron et al.
522   2012). A study using a mobile platform in the Unitah Basin found a clear aromatic source from the
523   condensate and water tanks on the gas well pads (Warneke et al. 2014).

524   Petron et al. (2012) implicated venting and condensate tanks in their assessment of benzene
525   emissions from O&NG operations, but noted that the benzene to propane ratios modeled from condensate
526   tank flashing and vented emissions was a factor of two lower than the benzene to propane ratios they
527   measured at BAO. The measured ratio BAO (10.1 ppt/ppb benzene/propane) is similar to the ratio of
528   benzene and propane measured in the canister samples from this work (0.011 ppb/ppb benzene/propane)
529   (Figure 7), an indication that the modeled condensate benzene emissions are too low and are not capturing
530   the full range of benzene being emitted during this process. This indicates that the O&NG processes
531   responsible for benzene in the WGF are still not well understood.

532   **Conclusions**

533   A PTR-MS quadrupole instrument collected continuous VOC time series data at PAO in the WGF
534   as part of the 2014 July-August DISCOVER-AQ field campaign. The interpretation of VOC measurements
535   is supported by meteorology and general AQ monitoring collected at minute resolution, as well as
536   compressed air canister samples collected during flight days. In addition to the ground based measurements
537   32 vertical profiles of VOCs measured by PTR-MS were collected over the site.

538   Unexpectedly high mixing ratios of benzene were observed at PAO during this study. The lowest
539   mixing ratios occurring the daytime, while the general nighttime increases in benzene was attributed to a
540   low nocturnal boundary layer. The high nighttime mixing ratios greatly increased the statistics for the site,
541   and indicate a much larger benzene pollution problem than was suspected in the area. VOC monitoring in
542   the WGF has primarily been conducted only during the daytime, and the high nighttime mixing ratios are
543   pushing up the benzene to levels that are a concern for public health. In addition the ground measurements,
544   aircraft measurements provided profiles of benzene and related compounds. These vertical diurnal profiles
545   over PAO indicate that the benzene originates from a local ground source rather than being transported to
546   the site, indicating that at short range O&NG benzene sources are more important than the more remote
547   Denver signal.

548   Canister samples collected at the surface during the aircraft profiles allowed for general source
549   signatures to be examined. Acetylene and propane were used as tracers for urban and natural gas sources.
550   The PAO canisters showed an overall strong natural gas signature, similar to canister results collected at a
551   nearby site in 2013; this was inferred from the i-pentane to n-pentane ratio. Additionally, acetylene and
552   propane used as a tracer against benzene indicate that, whereas there are multiple sources for benzene
553   measured in the canister samples at PAO, natural gas is a stronger source than the traffic sources.

554   Polar frequency analysis of the benzene measured in the PTR-MS shows that there is a directional
555   component to the benzene mixing ratios. The highest mixing ratios are associated with the SW wind regime,
556   while elevated mean and median benzene originates from the W and SW. This is a notable result because
557   it indicates we are observing a directional source rather than an increase in background benzene in the gas
558   field. Additionally, the high benzene measured from the SW at PAO corresponds to high benzene measured
559   in previous studies at BAO, which saw elevated benzene mixing ratios from the NE at BAO. The

560 observation of this SW benzene source is a more certain spatial constraint on the benzene source in the
561 WGF.

562   In prior work based in the WGF the major benzene sources in the gas field have been attributed to
563 a combination of combustion engines and natural gas extraction. However, the benzene to CO ratios
564 measured at PAO are unexpectedly high, even compared to the high ratio of benzene to CO measured at
565 BAO and attributed to gas field benzene production (Petron et al., 2012; Swarthout et al., 2013).The most
566 likely sources of benzene at PAO are condensation tanks and fugitive emissions of benzene from natural
567 gas operations in the Platteville area; the most likely source of CO is a non-combustive industrial process
568 to the SW of the site. However, to better resolve the benzene source question we need more directed
569 measurements around the natural gas infrastructure in the region and long term stationary measurements
570 deep in the WGF.

588   **References**

589   Adgate, J.L., Goldstein, B.D., McKenzie, L.M., 2014. Potential Public Health Hazards, Exposures and
590   Health Effects from Unconventional Natural Gas Development. Environmental Science &
591   Technology 48, 8307–8320. doi:10.1021/es404621d
592   Air emssions case study related to oil and gas development in Erie, Colorado, 2012. , Air Pollution
593   Control Division Technical Services Program. Colorado Department of Public Health and
594   Environment (CDPHE).
595   Allison, W., 2015. State of Colorado Comments, Docket ID EPA-HQ-OAR-2008-0699; FRL-9918-43-
596   OAR.
597   Apel, E.C., Emmons, L.K., Karl, T., Flocke, F., Hills, A.J., Madronich, S., Lee-Taylor, J., Fried, A.,
598   Weibring, P., Walega, J., Richter, D., Tie, X., Mauldin, L., Campos, T., Weinheimer, A., Knapp,
599   D., Sive, B., Kleinman, L., Springston, S., Zaveri, R., Ortega, J., Voss, P., Blake, D., Baker, A.,
600   Warneke, C., Welsh-Bon, D., de Gouw, J., Zheng, J., Zhang, R., Rudolph, J., Junkermann, W.,
601   Riemer, D.D., 2010. Chemical evolution of volatile organic compounds in the outflow of the
602   Mexico City Metropolitan area. Atmospheric Chemistry and Physics 10, 2353–2375.
603   doi:10.5194/acp-10-2353-2010
604   Apel, E.C., Hornbrook, R.S., Hills, A.J., Blake, N.J., Barth, M.C., Weinheimer, A., Cantrell, C.,
605   Rutledge, S.A., Basarab, B., Crawford, J., Diskin, G., Homeyer, C.R., Campos, T., Flocke, F.,
606   Fried, A., Blake, D.R., Brune, W., Pollack, I., Peischl, J., Ryerson, T., Wennberg, P.O., Crounse,
607   J.D., Wisthaler, A., Mikoviny, T., Huey, G., Heikes, B., O'Sullivan, D., Riemer, D.D., 2015. Upper
608   tropospheric ozone production from lightning NOx-impacted convection: Smoke ingestion case
609   study from the DC3 campaign. Journal of Geophysical Research: Atmospheres 120, 2505–2523.
610   doi:10.1002/2014JD022121
611   Baker, A.K., Beyersdorf, A.J., Doezema, L.A., Katzenstein, A., Meinardi, S., Simpson, I.J., Blake, D.R.,
612   Sherwood Rowland, F., 2008. Measurements of nonmethane hydrocarbons in 28 United States
613   cities. Atmospheric Environment 42, 170–182. doi:10.1016/j.atmosenv.2007.09.007
614   Bar-Ilan, A., Grant, J., Friesen, R., Pollack, A., Henderer, D., Pring, D., Sgamma, K., 2008. Development
615   of baseline 2006 emissions from oil and gas activity in the Denver-Julesburg Basin. ENVIRON
616   International Corporation.
617   Barletta, B., Meinardi, S., Simpson, I.J., Khwaja, H.A., Blake, D.R., Rowland, F.S., 2002. Mixing ratios
618   of volatile organic compounds (VOCs) in the atmosphere of Karachi, Pakistan. Atmospheric
619   Environment 36, 3429–3443.
620   Bloomdahl, R., Abualfaraj, N., Olson, M., Gurian, P.L., 2014. Assessing worker exposure to inhaled
621   volatile organic compounds from Marcellus Shale flowback pits. Journal of Natural Gas Science
622   and Engineering 21, 348–356. doi:10.1016/j.jngse.2014.08.018
623   Borbon, A., Gilman, J.B., Kuster, W.C., Grand, N., Chevaillier, S., Colomb, A., Dolgorouky, C., Gros,
624   V., Lopez, M., Sarda-Esteve, R., Holloway, J., Stutz, J., Petetin, H., McKeen, S., Beekmann, M.,
625   Warneke, C., Parrish, D.D., de Gouw, J.A., 2013. Emission ratios of anthropogenic volatile organic
626   compounds in northern mid-latitude megacities: Observations versus emission inventories in Los
627   Angeles and Paris: VOC EMISSION RATIOS IN MODERN MEGACITIES. Journal of
628   Geophysical Research: Atmospheres 118, 2041–2057. doi:10.1002/jgrd.50059
629   Bravo, H., Sosa, R., Sánchez, P., Bueno, E., González, L., 2002. Concentrations of benzene and toluene
630   in the atmosphere of the southwestern area at the Mexico City Metropolitan Zone. Atmospheric
631   Environment 36, 3843–3849.
632   Broderick, B.M., Marnane, I.S., 2002. A comparison of the C 2–C 9 hydrocarbon compositions of
633   vehicle fuels and urban air in Dublin, Ireland. Atmospheric Environment 36, 975–986.
634   Bunch, A.G., Perry, C.S., Abraham, L., Wikoff, D.S., Tachovsky, J.A., Hixon, J.G., Urban, J.D., Harris,
635   M.A., Haws, L.C., 2014. Evaluation of impact of shale gas operations in the Barnett Shale region
636   on volatile organic compounds in air and potential human health risks. Science of The Total
637   Environment 468-469, 832–842. doi:10.1016/j.scitotenv.2013.08.080

638   Burstyn, I., You, X. (Isabelle), Cherry, N., Senthilselvan, A., 2007. Determinants of airborne benzene
639   concentrations in rural areas of western Canada. Atmospheric Environment 41, 7778–7787.
640   doi:10.1016/j.atmosenv.2007.06.011
641   Buzcu-Guven, B., Olaguer, E.P., Herndon, S.C., Kolb, C.E., Knighton, W.B., Cuclis, A.E., 2013.
642   Identification of the source of benzene concentrations at Texas City during SHARP using an adjoint
643   neighborhood-scale transport model and a receptor model. Journal of Geophysical Research:
644   Atmospheres 118, 8023–8031. doi:10.1002/jgrd.50586
645   Capleton, A.C., Levy, L.S., 2005. An overview of occupational benzene exposures and occupational
646   exposure limits in Europe and North America. Chemico-Biological Interactions 153-154, 43–53.
647   doi:10.1016/j.cbi.2005.03.007
648   Chambers, A.K., Strosher, M., Wootton, T., Moncrieff, J., McCready, P., 2008. Direct Measurement of
649   Fugitive Emissions of Hydrocarbons from a Refinery. Journal of the Air & Waste Management
650   Association 58, 1047–1056. doi:10.3155/1047-3289.58.8.1047
651   Colborn, T., Kwiatkowski, C., Schultz, K., Bachran, M., 2011. Natural Gas Operations from a Public
652   Health Perspective. Human and Ecological Risk Assessment: An International Journal 17, 1039–
653   1056. doi:10.1080/10807039.2011.605662
654   de Gouw, J.A., Middlebrook, A.M., Warneke, C., Goldan, P.D., Kuster, W.C., Roberts, J.M., Fehsenfeld,
655   F.C., Worsnop, D.R., Canagaratna, M.R., Pszenny, A.A.P., Keene, W.C., Marchewka, M.,
656   Bertman, S.B., Bates, T.S., 2005. Budget of organic carbon in a polluted atmosphere: Results from
657   the New England Air Quality Study in 2002. Journal of Geophysical Research 110.
658   doi:10.1029/2004JD005623
659   Denver Metro Area & North Front Range Ozone Action Plan, 2008. . Colorado Air Quality Control
660   Commission.
661   Eiceman, G.A., Davani, B., Ingram, J., 1986. Depth profiles for hydrocarbons and polycyclic aromatic
662   hydrocarbons in soil beneath waste disposal pits from natural gas production. Environmental
663   Science & Technology 20, 508–514. doi:10.1021/es00147a011
664   Fortin, T.J., Howard, B.J., Parrish, D.D., Goldan, P.D., Kuster, W.C., Atlas, E.L., Harley, R.A., 2005.
665   Temporal Changes in U.S. Benzene Emissions Inferred from Atmospheric Measurements.
666   Environmental Science & Technology 39, 1403–1408. doi:10.1021/es049316n
667   Gelencsér, A., Siszler, K., Hlavay, J., 1997. Toluene-benzene concentration ratio as a tool for
668   characterizing the distance from vehicular emission sources. Environmental science & technology
669   31, 2869–2872.
670   Gentner, D.R., Worton, D.R., Isaacman, G., Davis, L.C., Dallmann, T.R., Wood, E.C., Herndon, S.C.,
671   Goldstein, A.H., Harley, R.A., 2013. Chemical Composition of Gas-Phase Organic Carbon
672   Emissions from Motor Vehicles and Implications for Ozone Production. Environmental Science &
673   Technology 47, 11837–11848. doi:10.1021/es401470e
674   Gilman, J.B., Kuster, W.C., Goldan, P.D., Herndon, S.C., Zahniser, M.S., Tucker, S.C., Brewer, W.A.,
675   Lerner, B.M., Williams, E.J., Harley, R.A., Fehsenfeld, F.C., Warneke, C., de Gouw, J.A., 2009.
676   Measurements of volatile organic compounds during the 2006 TexAQS/GoMACCS campaign:
677   Industrial influences, regional characteristics, and diurnal dependencies of the OH reactivity.
678   Journal of Geophysical Research 114. doi:10.1029/2008JD011525
679   Gilman, J.B., Lerner, B.M., Kuster, W.C., de Gouw, J.A., 2013. Source Signature of Volatile Organic
680   Compounds from Oil and Natural Gas Operations in Northeastern Colorado. Environmental
681   Science & Technology 130125095522001. doi:10.1021/es304119a
682   Greater Wattenberg Area Baseline Study, 2007. . Colorado Oil and Gas Conservation Commission
683   (COGCC).
684   Gross, S.A., Avens, H.J., Banducci, A.M., Sahmel, J., Panko, J.M., Tvermoes, B.E., 2013. Analysis of
685   BTEX groundwater concentrations from surface spills associated with hydraulic fracturing
686   operations. Journal of the Air & Waste Management Association 63, 424–432.
687   doi:10.1080/10962247.2012.759166

688   Heeb, N.V., Forss, A.-M., Bach, C., Reimann, S., Herzog, A., Jäckle, H.W., 2000. A comparison of
689   benzene, toluene and C2-benzenes mixing ratios in automotive exhaust and in the suburban
690   atmosphere during the introduction of catalytic converter technology to the Swiss Car Fleet.
691   Atmospheric Environment 34, 3103–3116. doi:10.1016/S1352-2310(99)00446-X
692   Helmig, D., Thompson, C.R., Evans, J., Boylan, P., Hueber, J., Park, J.-H., 2014. Highly Elevated
693   Atmospheric Levels of Volatile Organic Compounds in the Uintah Basin, Utah. Environmental
694   Science & Technology 48, 4707–4715. doi:10.1021/es405046r
695   Katzenstein, A.S., Doezema, L.A., Simpson, I.J., Blake, D.R., Rowland, F.S., 2003. Extensive regional
696   atmospheric hydrocarbon pollution in the southwestern United States. Proceedings of the National
697   Academy of Sciences 100, 11975–11979.
698   Kemball-Cook, S., Bar-Ilan, A., Grant, J., Parker, L., Jung, J., Santamaria, W., Mathews, J., Yarwood,
699   G., 2010. Ozone Impacts of Natural Gas Development in the Haynesville Shale. Environmental
700   Science & Technology 44, 9357–9363. doi:10.1021/es1021137
701   LaFranchi, B.W., Pétron, G., Miller, J.B., Lehman, S.J., Andrews, A.E., Dlugokencky, E.J., Hall, B.,
702   Miller, B.R., Montzka, S.A., Neff, W., Novelli, P.C., Sweeney, C., Turnbull, J.C., Wolfe, D.E.,
703   Tans, P.P., Gurney, K.R., Guilderson, T.P., 2013. Constraints on emissions of carbon monoxide,
704   methane, and a suite of hydrocarbons in the Colorado Front Range using observations of 14CO2.
705   Atmospheric Chemistry and Physics 13, 11101–11120. doi:10.5194/acp-13-11101-2013
706   Martins, D.K., Stauffer, R.M., Thompson, A.M., Knepp, T.N., Pippin, M., 2012. Surface ozone at a
707   coastal suburban site in 2009 and 2010: Relationships to chemical and meteorological processes.
708   Journal of Geophysical Research 117. doi:10.1029/2011JD016828
709   McKenzie, L.M., Witter, R.Z., Newman, L.S., Adgate, J.L., 2012. Human health risk assessment of air
710   emissions from development of unconventional natural gas resources. Science of The Total
711   Environment 424, 79–87. doi:10.1016/j.scitotenv.2012.02.018
712   Moore, C.W., Zielinska, B., Pétron, G., Jackson, R.B., 2014. Air Impacts of Increased Natural Gas
713   Acquisition, Processing, and Use: A Critical Review. Environmental Science & Technology 48,
714   8349–8359. doi:10.1021/es4053472
715   Natural Gas Annual 2014, 2015. . Energy Information Administration.
716   Pétron, G., Frost, G., Miller, B.R., Hirsch, A.I., Montzka, S.A., Karion, A., Trainer, M., Sweeney, C.,
717   Andrews, A.E., Miller, L., Kofler, J., Bar-Ilan, A., Dlugokencky, E.J., Patrick, L., Moore, C.T.,
718   Ryerson, T.B., Siso, C., Kolodzey, W., Lang, P.M., Conway, T., Novelli, P., Masarie, K., Hall, B.,
719   Guenther, D., Kitzis, D., Miller, J., Welsh, D., Wolfe, D., Neff, W., Tans, P., 2012. Hydrocarbon
720   emissions characterization in the Colorado Front Range: A pilot study. Journal of Geophysical
721   Research 117. doi:10.1029/2011JD016360
722   Pétron, G., Karion, A., Sweeney, C., Miller, B.R., Montzka, S.A., Frost, G.J., Trainer, M., Tans, P.,
723   Andrews, A., Kofler, J., Helmig, D., Guenther, D., Dlugokencky, E., Lang, P., Newberger, T.,
724   Wolter, S., Hall, B., Novelli, P., Brewer, A., Conley, S., Hardesty, M., Banta, R., White, A., Noone,
725   D., Wolfe, D., Schnell, R., 2014. A new look at methane and nonmethane hydrocarbon emissions
726   from oil and natural gas operations in the Colorado Denver-Julesburg Basin: Hydrocarbon
727   emissions in oil & gas basin. Journal of Geophysical Research: Atmospheres 119, 6836–6852.
728   doi:10.1002/2013JD021272
729   Roberts, J.M., Fehsenfeld, F.C., Liu, S.C., Bollinger, M.J., Hahn, C., Albritton, D.L., Sievers, R.E., 1984.
730   Measurements of aromatic hydrocarbon ratios and NOx concentrations in the rural troposphere:
731   Observation of air mass photochemical aging and NOx removal. Atmospheric Environment (1967)
732   18, 2421–2432. doi:10.1016/0004-6981(84)90012-X
733   Seigneur, C., Pun, B., Lohman, K., Wu, S., 2003. Regional Modeling of the Atmospheric Fate and
734   Transport of Benzene and Diesel Particles. Environmental Science & Technology 37, 5236–5246.
735   doi:10.1021/es034433o
736   Swarthout, R.F., Russo, R.S., Zhou, Y., Hart, A.H., Sive, B.C., 2013. Volatile organic compound
737   distributions during the NACHTT campaign at the Boulder Atmospheric Observatory: Influence of

738   urban and natural gas sources. Journal of Geophysical Research: Atmospheres 118, 10,614–10,637.
739   doi:10.1002/jgrd.50722
740   Thompson, C.R., Hueber, J., Helmig, D., 2014. Influence of oil and gas emissions on ambient
741   atmospheric non-methane hydrocarbons in residential areas of Northeastern Colorado. Elementa:
742   Science of the Anthropocene 2, 000035. doi:10.12952/journal.elementa.000035
743   Verma, D.K., Johnson, D.M., McLean, J.D., 2000. Benzene and Total Hydrocarbon Exposures in the
744   Upstream Petroleum Oil and Gas Industry. AIHAJ - American Industrial Hygiene Association 61,
745   255–263. doi:10.1080/15298660008984534
746   Wallace, L.A., 1989. Major sources of benzene exposure. Environmental health perspectives 82, 165.
747   Warneke, C., Geiger, F., Edwards, P.M., Dube, W., Pétron, G., Kofler, J., Zahn, A., Brown, S.S., Graus,
748   M., Gilman, J.B., Lerner, B.M., Peischl, J., Ryerson, T.B., de Gouw, J.A., Roberts, J.M., 2014.
749   Volatile organic compound emissions from the oil and natural gas industry in the Uintah Basin,
750   Utah: oil and gas well pad emissions compared to ambient air composition. Atmospheric Chemistry
751   and Physics 14, 10977–10988. doi:10.5194/acp-14-10977-2014
752   Warneke, C., McKeen, S.A., de Gouw, J.A., Goldan, P.D., Kuster, W.C., Holloway, J.S., Williams, E.J.,
753   Lerner, B.M., Parrish, D.D., Trainer, M., Fehsenfeld, F.C., Kato, S., Atlas, E.L., Baker, A., Blake,
754   D.R., 2007. Determination of urban volatile organic compound emission ratios and comparison
755   with an emissions database. Journal of Geophysical Research 112. doi:10.1029/2006JD007930
756   World Health Organization (Ed.), 2000. Air quality guidelines for Europe, 2nd ed, WHO regional
757   publications. World Health Organization, Regional Office for Europe, Copenhagen.
758

759 **Tables**

760

761 Table 1. Spatial statistics for benzene measured over the collection sites from 3 km ASL and below.

	Fort Collins	Chatfield	NREL/Golden	BAO	Denver/La Casa	PAO
Mean	0.068	0.080	0.087	0.102	0.119	0.140
Median	0.064	0.071	0.085	0.095	0.110	0.115
25th	0.036	0.038	0.045	0.053	0.067	0.062
75th	0.095	0.110	0.122	0.139	0.166	0.190
Max	0.269	0.284	0.260	0.674	0.466	1.004

762

763 Table 2. Quantitative statistics for benzene measured at PAO, units in ppbv.

	Campaign	**Day**	**Night**
Mean	**0.53**	**0.37**	**0.74**
Median	**0.33**	**0.18**	**0.54**
25th	0.14	0.10	0.30
75th	0.66	0.45	0.89
Max	29.3	20.6	29.3

764

765 Table 3. Mean PAO toluene/benzene ratios by wind sector, with diurnal information.

Wind Sector	Total	Day	Night
N	1.26 ± 0.62	1.16 ± 0.81	1.37 ± 0.28
NE	1.32 ± 0.52	1.03 ± 0.40	1.55 ± 0.49
E	1.03 ± 0.42	0.88 ± 0.36	1.25 ± 0.40
SE	1.09 ± 0.71	0.97 ± 0.70	1.36 ± 0.65
S	1.41 ± 1.86	1.13 ± 1.22	1.61 ± 2.19
SW	1.34 ± 0.48	1.06 ± 0.71	1.41 ± 0.38
W	1.29 ± 0.43	0.95 ± 0.64	1.39 ± 0.26
NW	1.33 ± 0.46	1.21 ± 0.41	1.42 ± 0.27
Calm	1.32 ± 0.41	1.02 ± 0.56	1.39 ± 0.32

766

767 Table 4. PAO canister correlations compared to Platteville, CO, literature correlation values

|	Propane		Acetylene	
	Thompson et al. (2014)	PAO (2014)	Thompson et al. (2014)	PAO (2014)
n-butane	0.95	0.99	0.15	0.50
i-pentane	0.91	0.99	0.08	0.49
n-pentane	0.94	0.97	0.12	0.43
Benzene	0.73	0.70	0.29	0.27

768

769

770

771 **Figures**
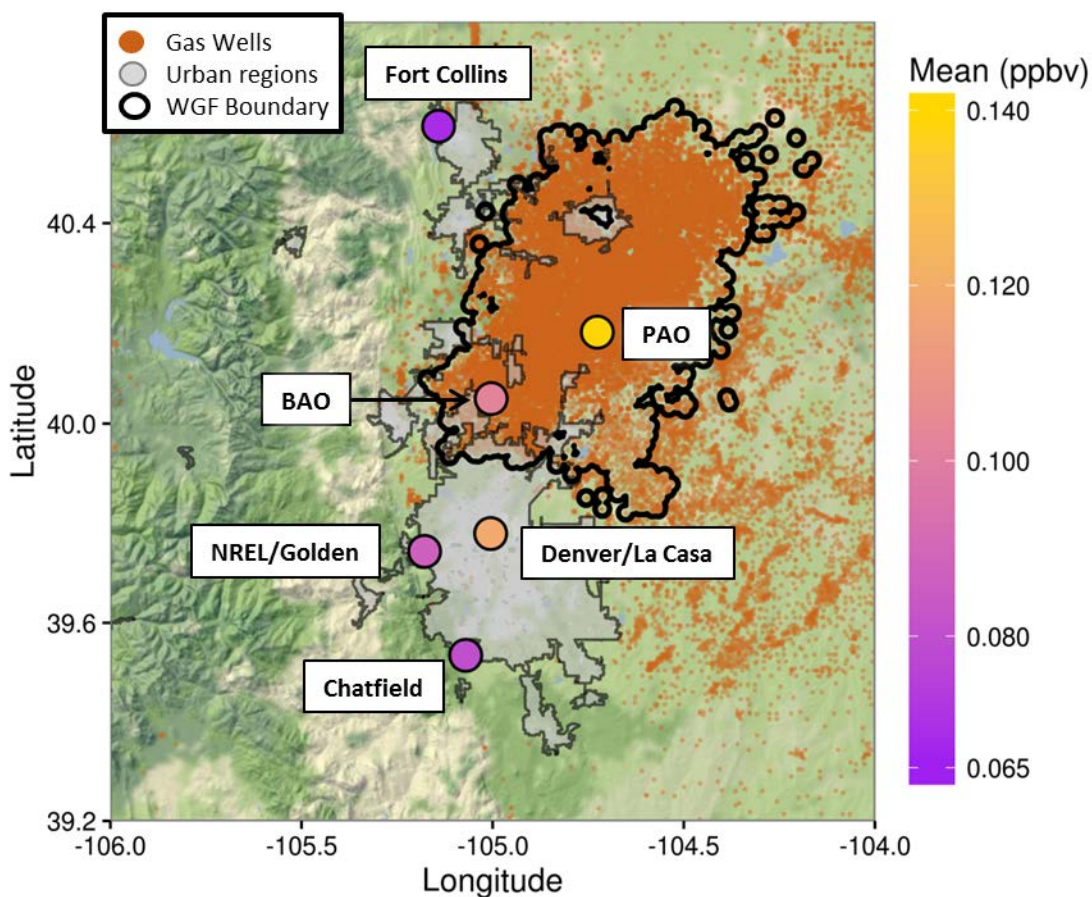
772

773 Figure 1. Map of the 2014 DISCOVER-AQ study area. The urban areas are shown in grey (data courtesy
774 of the United States Census Bureau, http://www.census.gov/geo/maps-data/data/tiger.html). The
775 boundary of the WGF is shown in black along with the gas wells (yellow points) (data courtesy of the
776 Colorado Oil and Gas Conservation Commission, http://cogcc.state.co.us/). The DISCOVER-AQ ground
777 sites are plotted and colored using the mean benzene measured from the aircraft spiral observations for
778 each sites. The benzene statistics were calculated using the bottom 1 km AGL for each site.
779
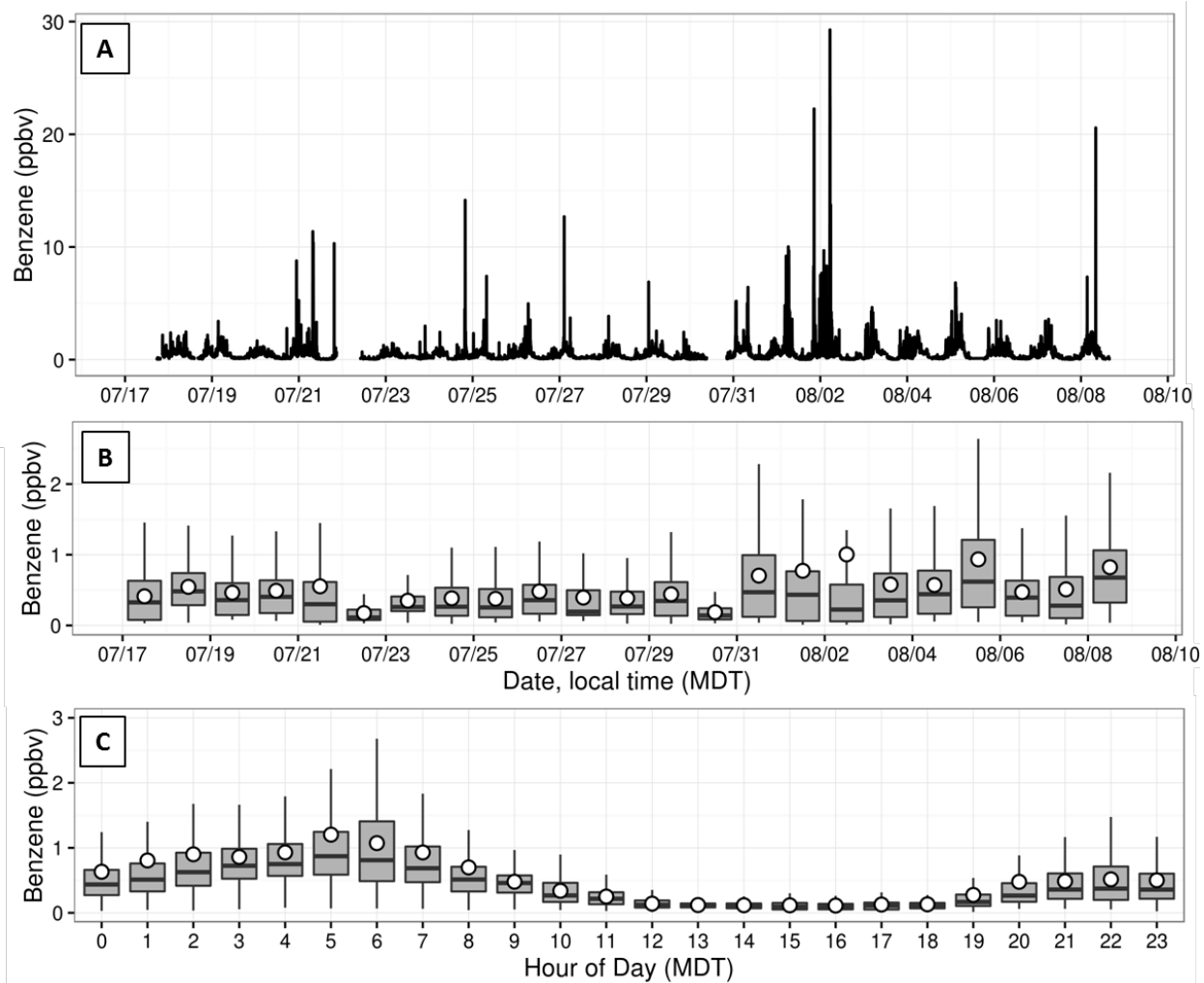
Figure 2. PTR-MS Benzene measurements collected at PAO during the campaign. A. The ground level benzene time series for the full campaign. B. Box and whisker benzene mixing ratios organized by day, midnight to midnight MDT. The outlier points are not shown. The open points are the daily means. C. The diurnal cycle of benzene over all observations. The outlier points are not shown for clarity, the open points are the hours mean values. All dates and times are in local (MDT) time.
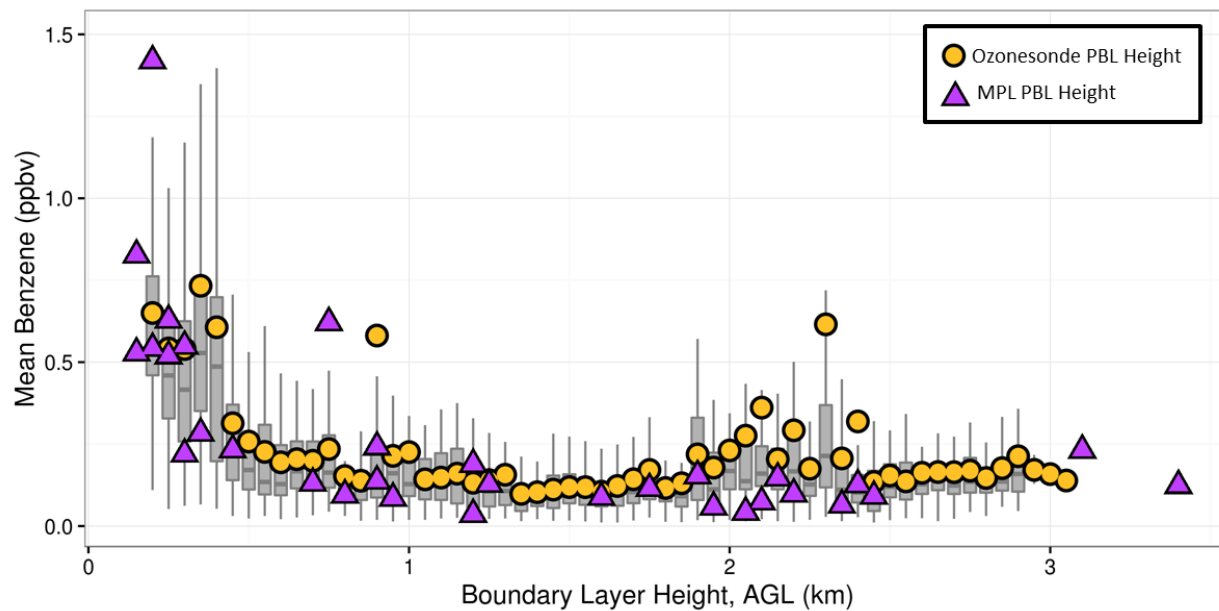
Figure 3. The Benzene relationship to PBLH high (AGL). The purple triangles are PBLH calculated from the ozonesondes launched at PAO, using 15 minute mean benzene data beginning from the launch time. The gold points are the mean aerosol MPL calculated PBLH binned by 50 m, collected between 0700 and 1900 MDT. The grey boxes are the statistical box and whisker plots for the MPL PBLH data. The outlier points for the box and whisker plots are excluded for clarity.
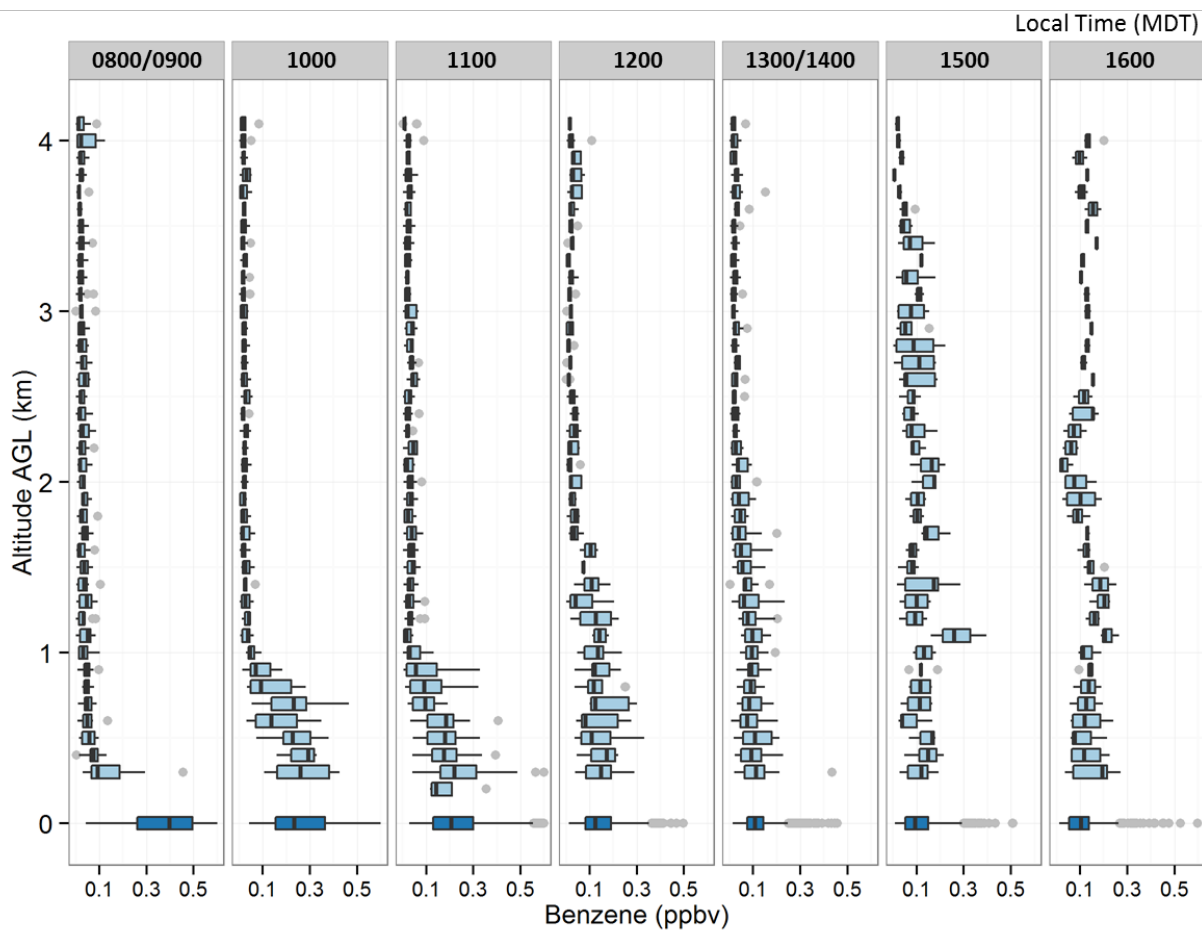
795
796 Figure 4. Vertical diurnal profiles of benzene over PAO. The aircraft data was binned into 50 m boxes
797 and plotted as a box and whiskers plot. The plot is further separated by hour of day (local time, MDT).
798 All benzene mixing ratios are cut off a 0.60 ppbv for clarity. A total of 29 total spirals and three partial
799 spirals were used to construct this plot.
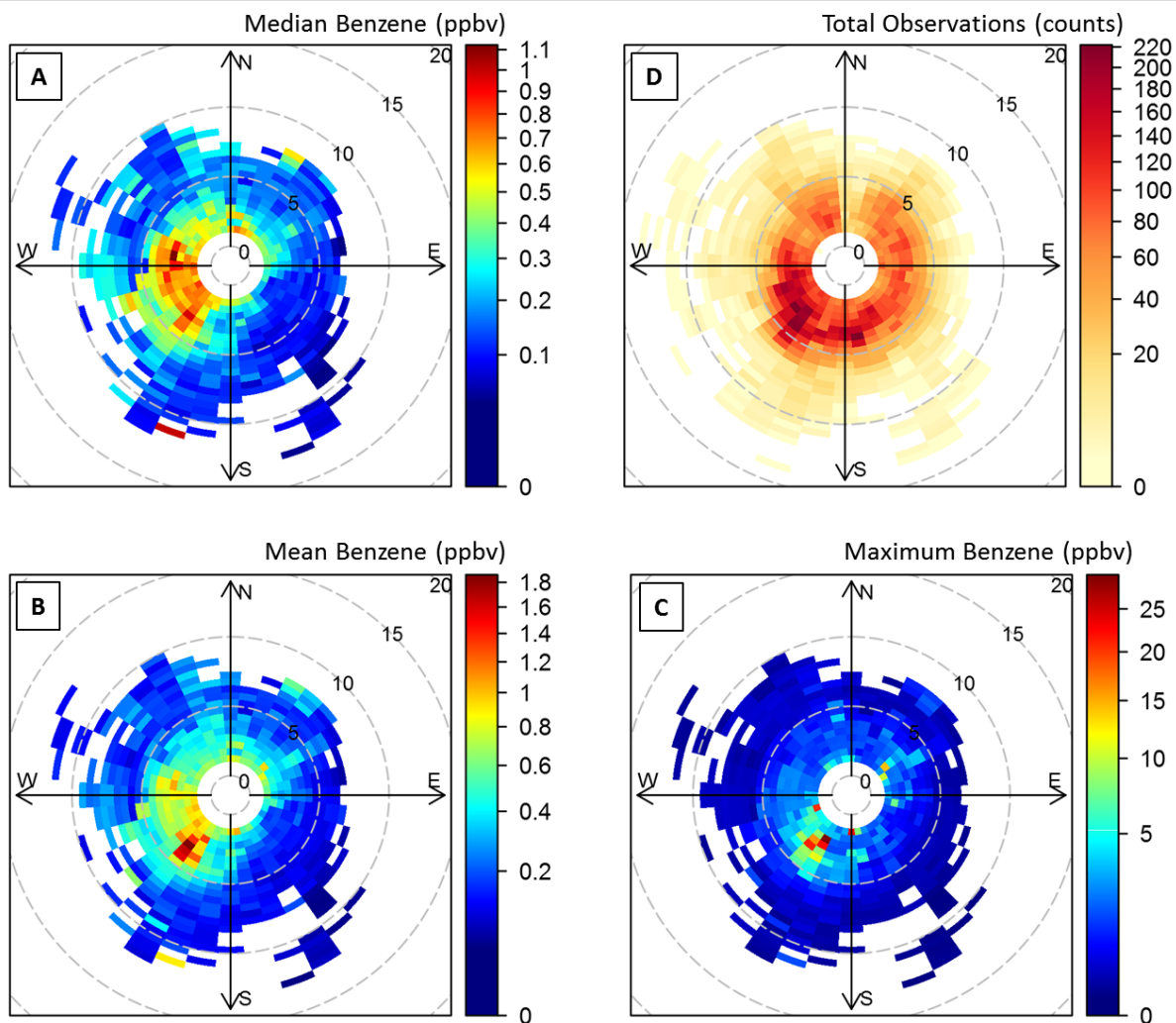
800
801 Figure 5. Total campaign polar frequency plots of benzene measured at PAO. The wind observations are
802 binned by 10 degrees wind direction and 0.5 m/s wind speed. The wind speed and direction bins are
803 plotted on a polar plot and colored based on the calculated statistic. Enhanced benzene has directional
804 dependence and is associated with SW flow over the site, especially in higher mixing ratios (mean,
805 maximum).
806

807
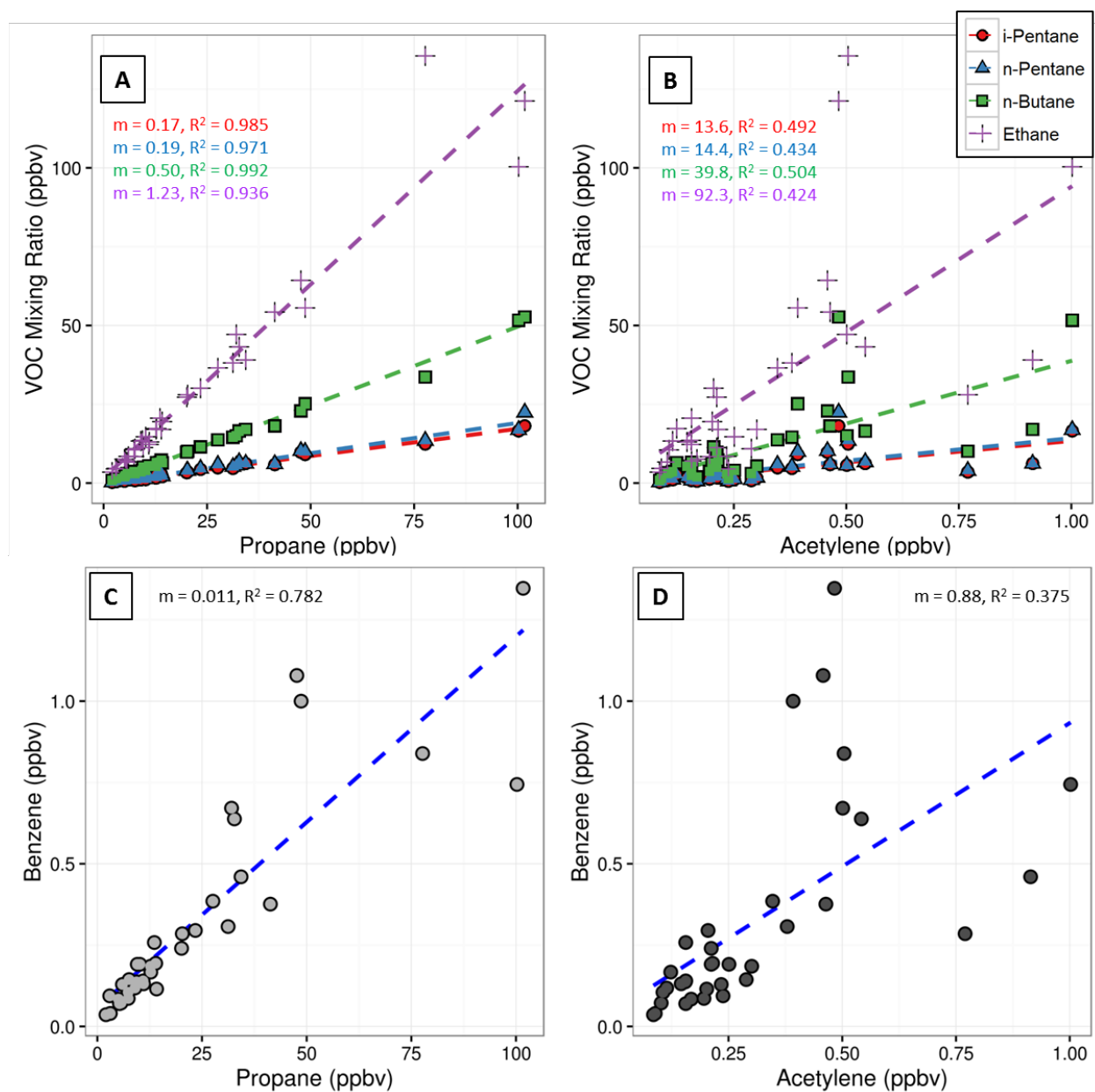
Figure 6. Canister VOC measurements of VOCs correlated with propane, an O&NG tracer, and acetylene, a traffic and combustion tracer. The combustion tracers i-pentane, n-pentane, n-butane and ethane show a a stronger correlation with proane (A) than with acetylene (B), indicating a strong O&NG influence at PAO. Benzene also shows a strong correlation with propane (C) over acetylene (D), although the correlations with benzene in general have lower correlation constants compared to the combustion tracers.
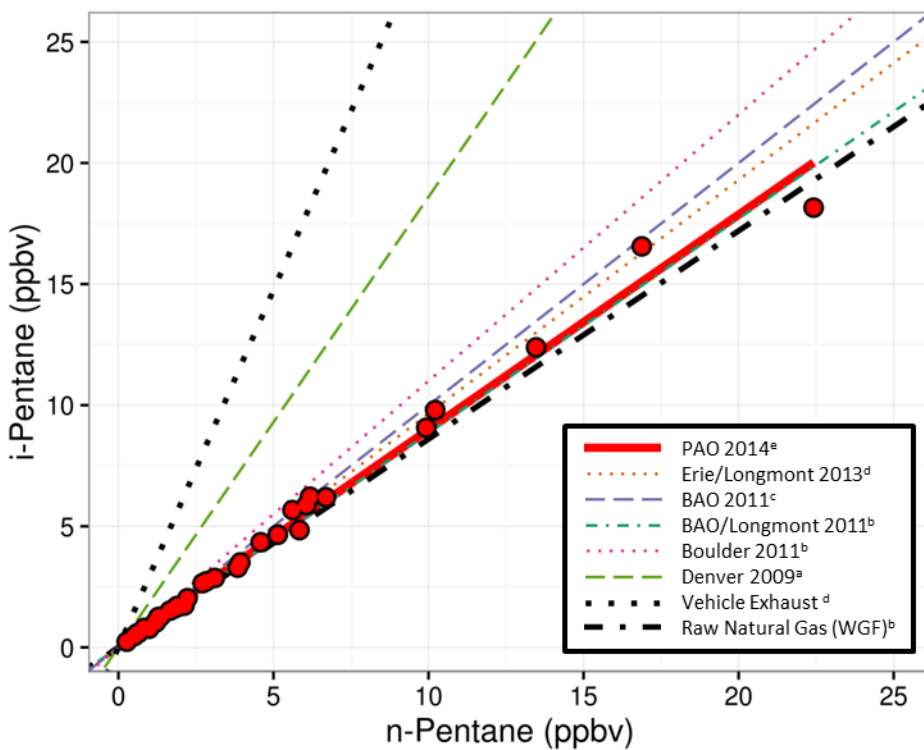
Figure 7. Canister VOC measurements of i-pentane and n-pentane during the campaign, and literature ratios from NE Colorado studies. ([a]Baker et al., 2009; [b]Gilman et al., 2013; [c]Swarthout et al. 2013; [d]Thompson et al., 2014; [e]This work, 2016)
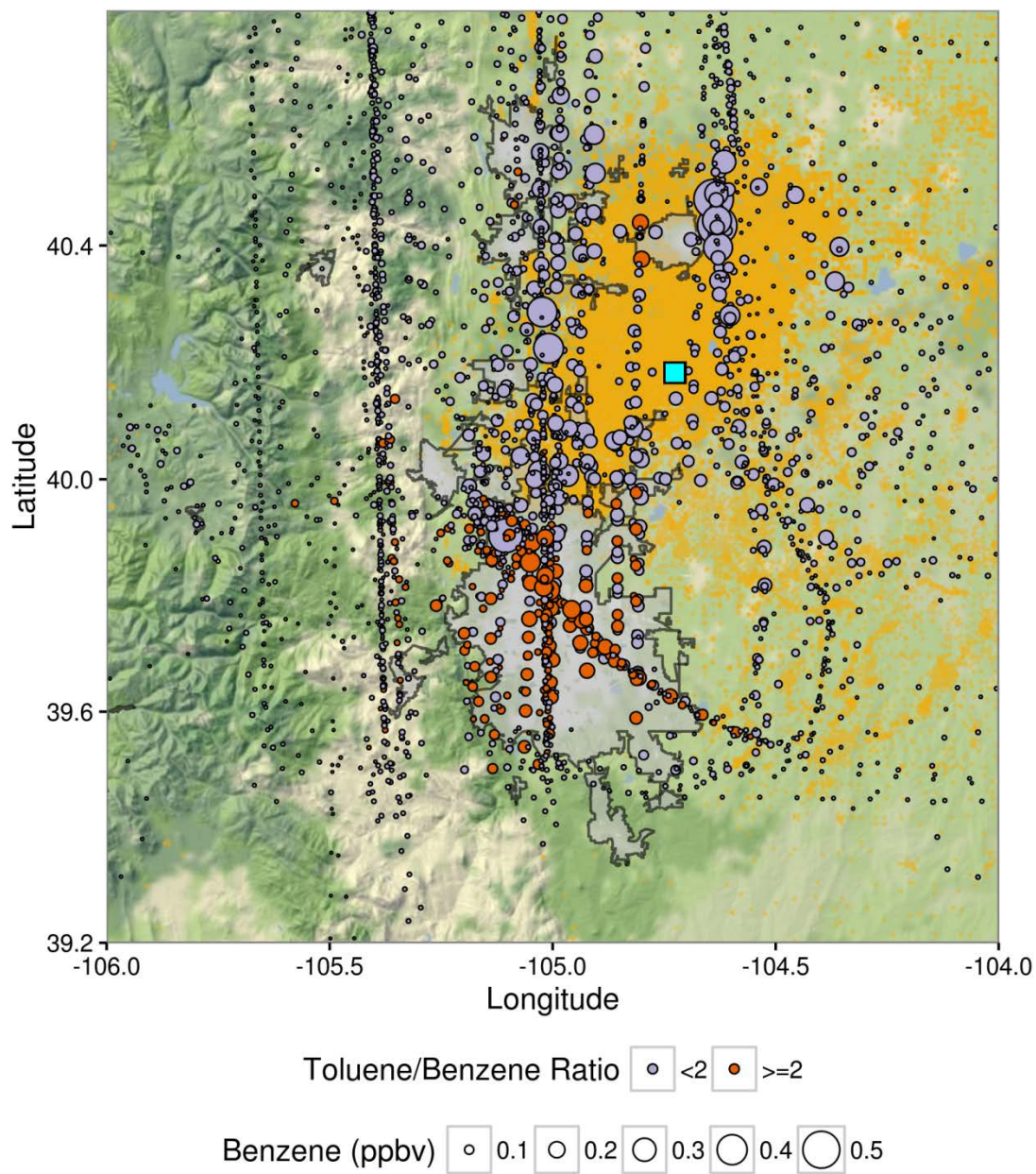
Figure 8. Toluene to benzene spatial ratios calculated from the FRAPPE C-130 TOGA data. The data points over the map are colored by the toluene to benzene ratio, and sized by the measured benzene mixing ratio at each observation. PAO is marked with a cyan square.
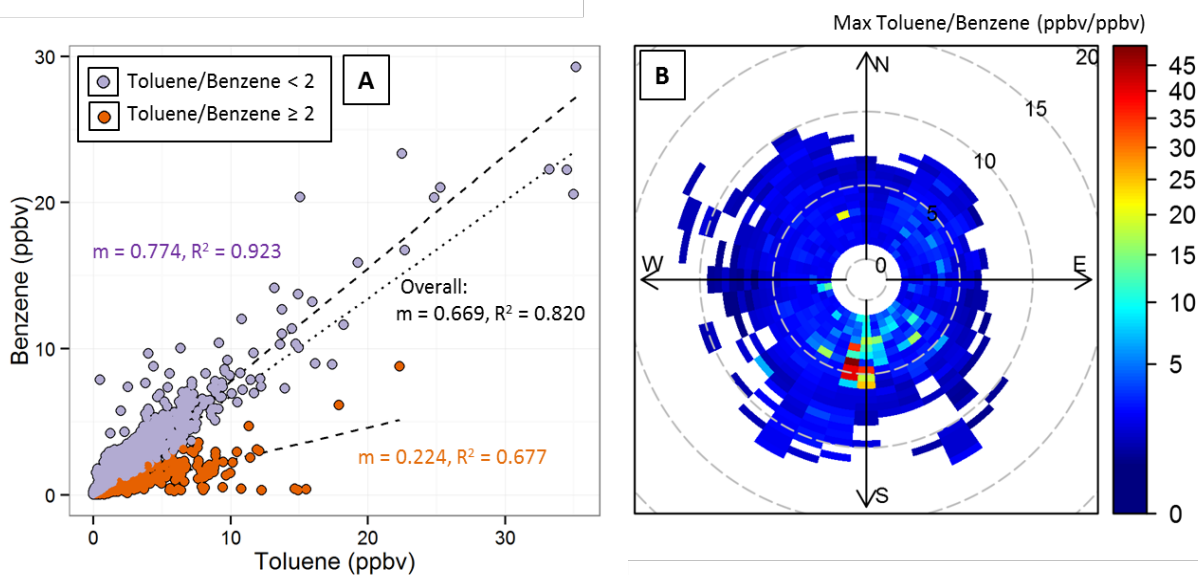
827
828 Figure 9. Toluene to benzene correlation from the PTR-MS data. A. The correlation plot of benzene to
829 toluene for the full campaign. The points are color coded by the toluene/benzene ratio. A toluene/benzene
830 ratio ≥ 2 is associated with fresh vehicle emissions and/or vehicles without catalytic converters. B. a polar
831 frequency plot of the toluene/benzene ratio shows that these high ratio observations are associated with
832 southerly winds.
833
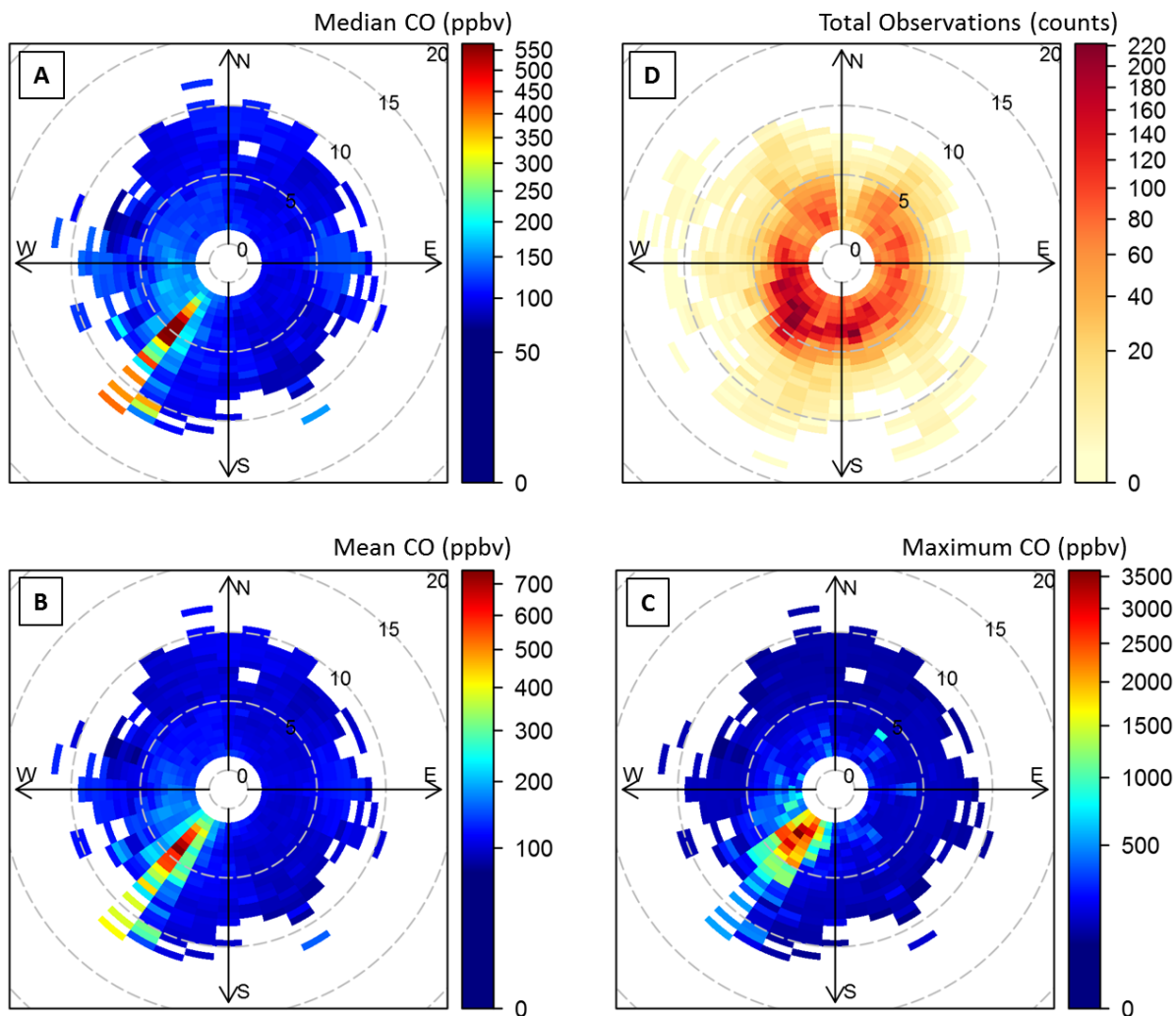
834

835 Figure 10. Total campaign polar frequency plots of CO measured at PAO. The wind observations are
836 binned by 10 degrees wind direction and 0.5 m/s wind speed. Enhanced CO has directional dependence
837 associated with SW flow over the site, similar to the results for benzene (Figure 4). CO has a stronger
838 wind direction dependence, indicative of a point source located in close proximity to PAO.
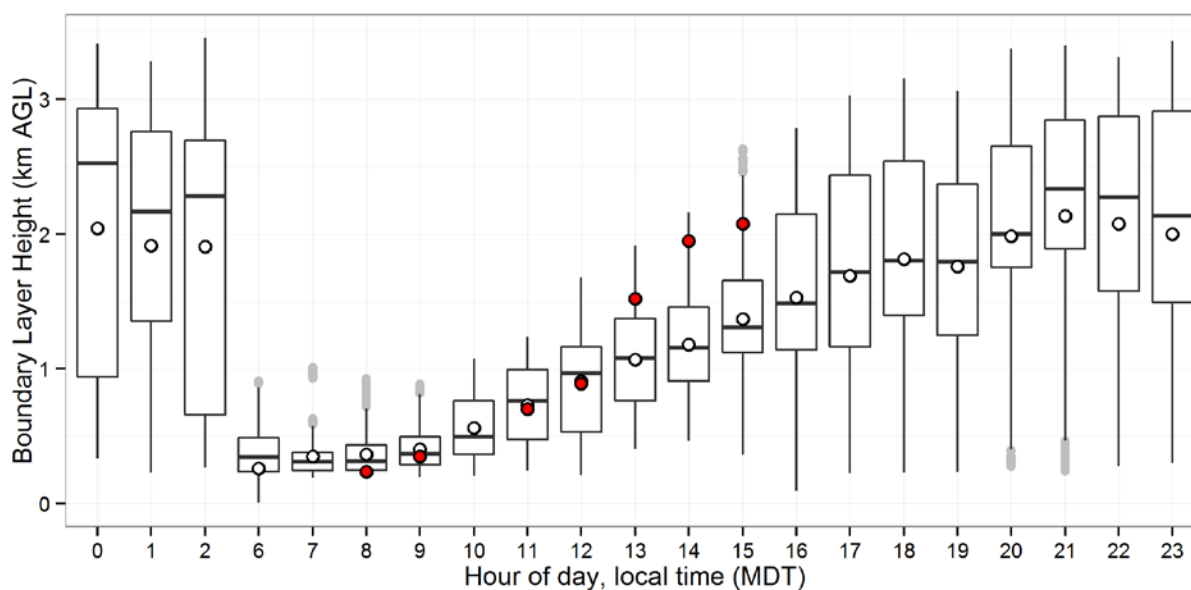
839
840
841
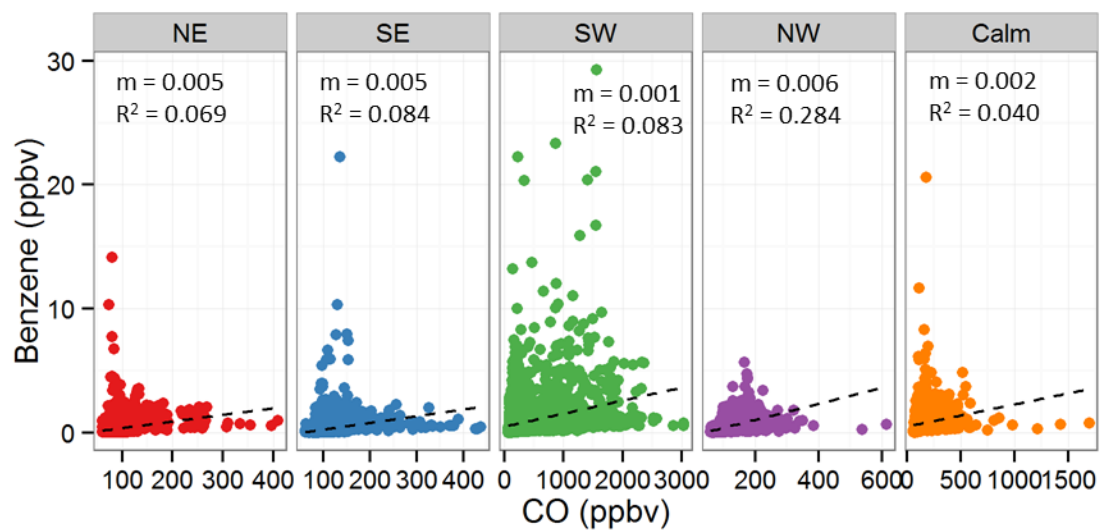
Figure 11. Benzene-CO correlations for all observations, faceted by general wind direction. Calm winds had a measured wind speed less than 1 m/s for the minute average.

842

843

844

845

846   **Supplementary Figures**

847
848   Supplementary Figure 1. PBLH diurnal profile. The box and whisker plots are created from the MPL
849   PBLH calculations from 22 July 2014 through the end of 11 August 2014. The open points show mean
850   MPL PBLH for each hour. The red points show mean ozonesonde PBLH for each hour. At 1000 MDT
851   both the mean and the median of the PBLH calculated from the MPL are ≥ 0.5 Km AGL, making 1000
852   MDT the beginning of the daytime-type boundary layer.
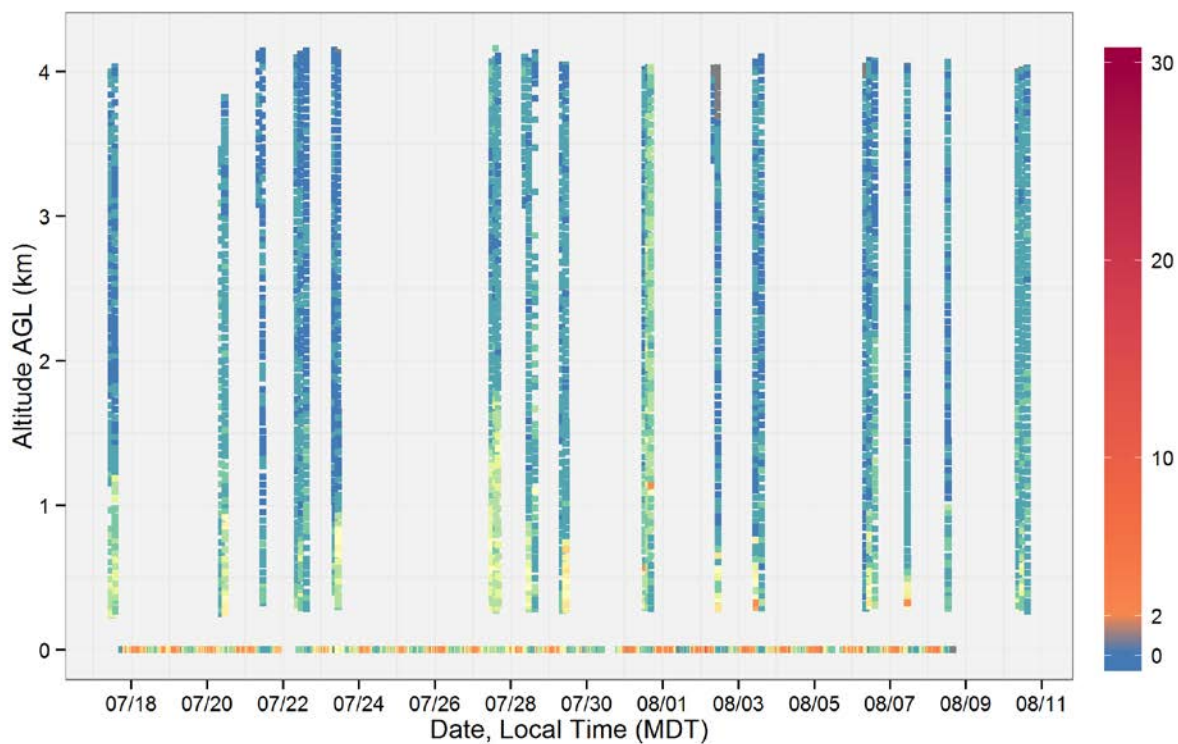
853
854   Supplementary Figure 2. Vertical benzene profiles and ground benzene measurements collected at PAO
855   during the study. Each point is plotted based on the time stamp and GPS altitude data from the P3-B
856   spirals. The altitudes are reported above ground level (AGL). Each point is colored by measured benzene
857   mixing ratio. Low aircraft measurements of benzene contrast with the high ground benzene measured
858   throughout the campaign.
859
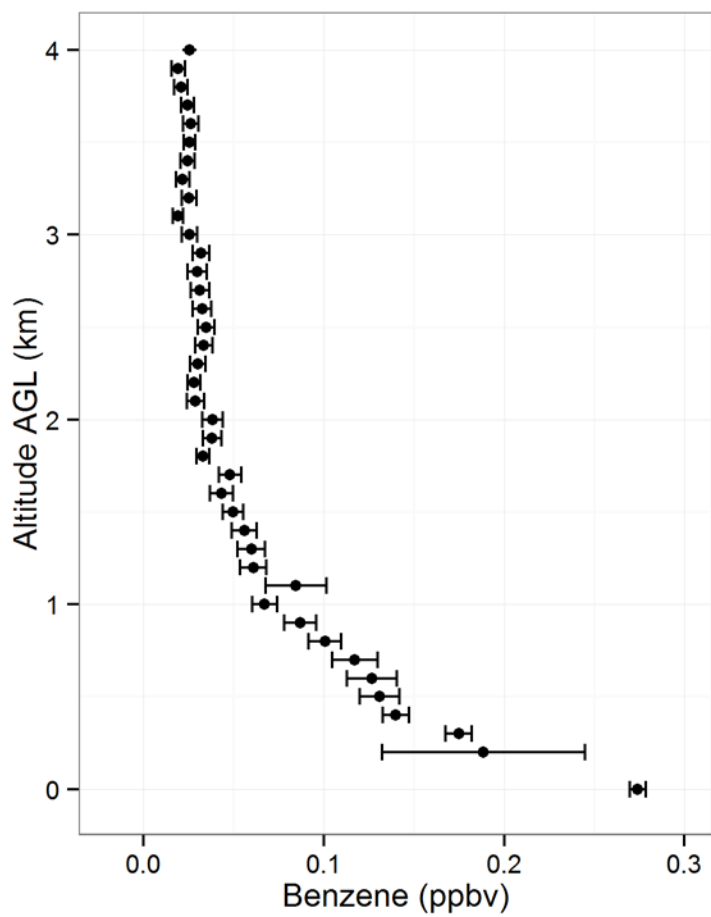
860

861   Supplementary Figure 3. Benzene mean profile over PAO from the vertical aircraft spirals. The points are
862   the mean mixing ratios binned by 50 m bins. The error bars show the standard deviation of the mean for
863   each vertical bin.
864

865
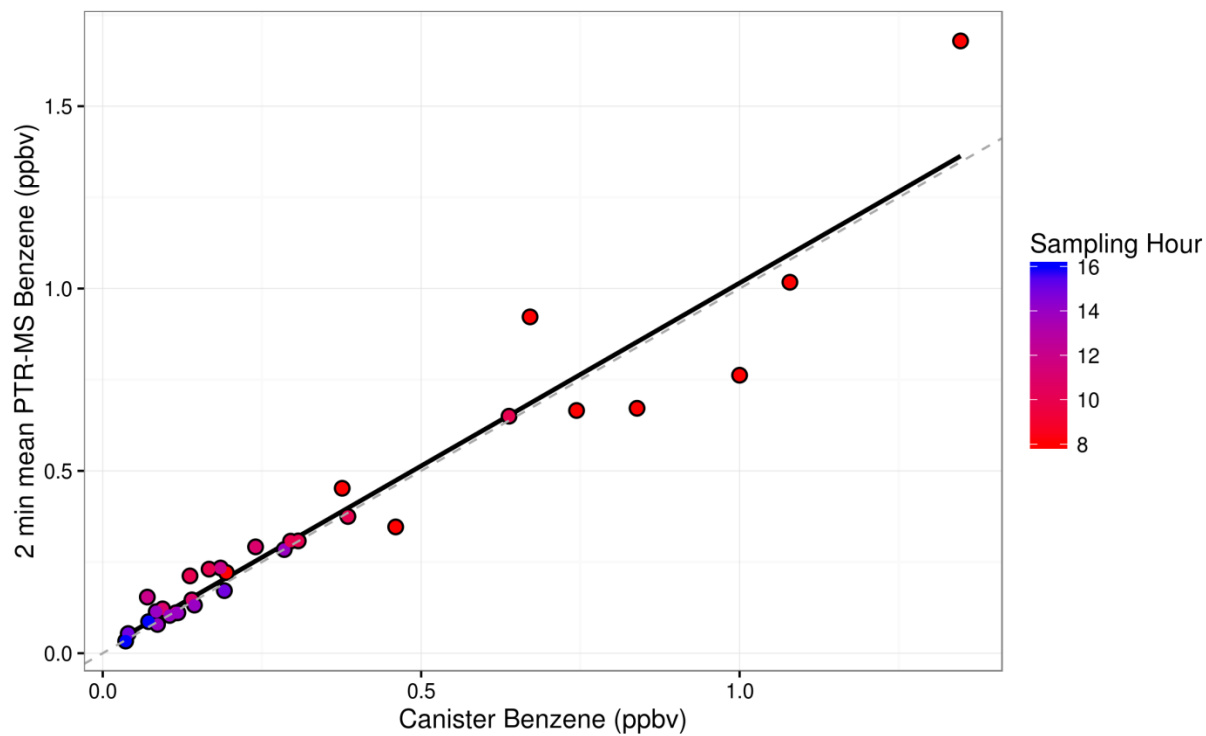
Supplementary Figure 4. Canister benzene correlated with 2min mean benzene, with the mean benzene
window centered on the canister opening time. The grey dashed line shows the 1-to-1 line. The black
lines shows the linear regression best fit line, which has a slope of 1.003, and $R^2 = 0.9205$. The points are
colored by their hour of collection, in local time (MDT).

870
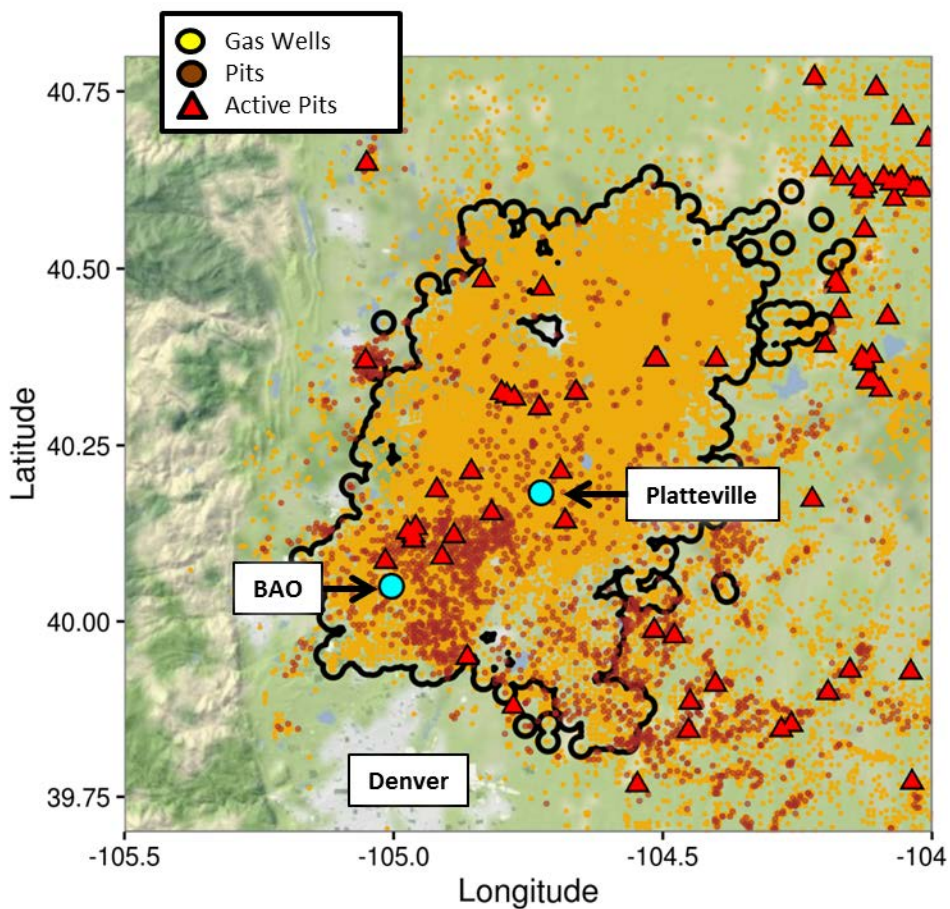
Supplementary Figure 5. Waste pit locations and statuses provided by COGCC. The cyan points show the locations of the PAO and BAO sampling sites for the campaign. The black outline shows the political boundary of the WGF as defined by the COGCC. The red triangles show the locations of the active waste pit locations as reported from the COGCC data.